2005

Infrared Thermography And High Accuracy Gps For Automated Asphalt Crack Detection

Tarek M. Abdel-Monem
University of Central Florida

INFRARED THERMOGRAPHY AND HIGH ACCURACY GPS FOR AUTOMATED ASPHALT CRACK DETECTION

by

TAREK ABDEL-MONEM
B.S. University of Alexandria, Egypt, 1986

A thesis submitted in partial fulfillment of the requirements
for the degree of Master of Science
in the Department of Civil and Environment Engineering
in the College of Engineering and Computer Science
at the University of Central Florida
Orlando, Florida

Summer Term
2005

ABSTRACT

Roads are major public assets. The USA spends billions of dollars each year on road construction and maintenance. To keep these roads in a healthy condition and for better planning and allocation of maintenance budgets, knowledge of distressed locations is needed. Roads develop cracks when they are subjected to stresses that exceed their designed criteria or their materials properties. Early detection and repair of cracks has proven to be the most cost-effective strategy in limiting the damage to roads and reducing expenditures.

Various methodologies of crack detection were developed and significant techniques were made in the last few years. One of the most important recent technologies is the infrared thermography, which allows the use of infrared waves for crack detection. Another important technology is the global navigation satellite system (GNSS) which currently includes the GPS and GLONASS constellations. With the help of these systems, accurate location coordinates (longitude, latitude and altitude) up to a few centimeters were located.

The objective of this research is to test the combined use of GNSS and infrared thermography in an automated system for the detection of asphalt cracks and their locations. To achieve this goal, two tests have been conducted. The first one, regarding the location tagging, was done using two pairs of GPS receivers which can detect signals from both GPS and GLONASS navigation systems in single and dual frequencies (L1 and L2). Different modes have been set to the receiver and comparison graphs were developed to compare accuracies against modes. The second test involves an infrared camera mounted on a car and moving in speeds approaching highway speed limit. The images obtained from the camera were processed using cracks detection software to analyze cracks properties (length, width, density and severity).

It was found that the images that were taken by a moving infrared camera were recognized by crack detection software for moving speeds up to 50 mph. At speeds higher than 50 mph, images were blurred. As for location test, The GLONASS combined by GPS receivers got slightly better results than GPS only in both dual and single frequencies. The GLONASS satellites are not always available in view and when they are there, the number of satellites that can be detected by receiver range from one to three satellites at the most and for only a short period of time.

It is recommended that future research be conducted to investigate the effect of using different camera lenses on the clarity of the images obtained as well as the effect of raising the camera level above the pavement surface in such a way that the whole lane width (12 ft.) would be covered in one image. Also the total reliance on GPS only receivers in determining cracks location has proven to be enough for this application.

ACKNOWLEDGMENTS

I would like to express my sincere thanks to my advisor, Prof. Amr Oloufa, for giving me such a great opportunity to work with him in this research. His guidance and encouragement were of great help to complete my degree. I would like to express my gratitude to Prof. Yasser Hosni for his great support and valuable advice during my study at UCF. I also wish to thank Prof. Shiou-San Kuo for acting on my committee and his valuable time to review my thesis.

I wish to thank Dr. Hesham Mahgoub for his help during the thesis, and for his helpful advice. I am very grateful to my colleague Ms. Engy Serag for her knowledge and her support.

Special thanks to Mr. John G. Fricot, of FLIR Systems Inc., for providing the hardware used for infrared investigation. I appreciate the assistance of Mr. Yanbo Zhou of Roadware Inc. for his valuable software assistance.

Finally, I sincerely wish to thank my wife, my sister and my kids for giving the chance and the environment to complete this work.

TABLE OF CONTENTS

LIST OF FIGURES

LIST OF TABLES

LIST OF ACRONYMS

DOT	Department of Transportation
GLONASS	Global Navigation Satellite System (Russian)
GNSS	Global Navigation Satellite System
GPR	Ground Penetration Radar
GPS	Global Positing System
IR	Infrared
PPS	Precise Positioning Service
PRN	Pseudo Random Noise
RTK	Real Time Kinematic
SPS	Standard Positioning Service

1. INTRODUCTION

1.1 Background

Monitoring and evaluating roads` condition is a major factor for keeping infrastructure in a healthy condition. Roads construction and maintenance consumes billions of dollars in the USA each year. The early detection and remedial of roads` distressed locations would help in minimizing the maintenance cost, better planning for allocating the maintenance budgets, and to keep the traffic running smoothly and safely.

Roads` distressed areas may occur from a variety of reasons ranging from improper assumptions for some of the designing criteria during the design phase, to deficiencies in construction materials or methods during the construction phase. Some other reasons maybe natural or cannot be predicted such as sinkholes or damage to underlying utility pipelines. So, when roads are loaded with traffic, it causes stresses that exceed their capacity and lead to cracks. Furthermore, water from rain flows into these cracks washes away fines, causing settlement, aggravating the condition of the distressed area and eventually leads to surface breakup.

1.2 Problem Statement

Two important concepts should be taken into consideration in any crack detection system; the identification of the cracks (type, width, length and severity) and the determination of their exact location. Over the past years many methods for pavements cracks detection have been developed and used, beginning with visual observation to automated systems that utilize

analog or digital cameras and crack detection software. However, human visual inspections are impractical (time-wise) and very costly. The analog and digital cameras are limited to certain weather conditions and they need ample amount of light to work properly.

As for the cracks locations, mapping methods use traditional surveying equipment or using reference stations. These methods are labor intensive and suffer from man-made errors, making it hard to track back to the exact crack location.

The ideal crack detection system should be able to detect all asphalt cracks types of small sizes under all weather conditions with reasonable speed (has no impact on the running traffic), while determining the exact location coordinates of detected crack.

Various methodologies of crack detection were developed and significant techniques were implemented in the past few years. One of the most important recent technologies is the infrared thermography, which allows the use of infrared waves for crack detection. Another important technology is the global navigation satellite system (GNSS) which currently includes the GPS and GLONASS constellations. With the help of these systems, accurate coordinates locations' (longitude, latitude and altitude) up to a few centimeters were detected.

1.3 Research Objective

The purpose of this study is to integrate infrared thermography technology and the GNSS systems in identifying the asphalt cracks and to determine their precise location. Two important aspects were studied in this research:

1. The feasibility of using infrared camera to capture images on speeds near to highway speeds that can be processed and analyzed by crack detection software.

2. The selection of the suitable GPS / GLONASS receiver parameters that can provide the crack location with practical level of accuracy.

The system should be considered as a proof of concept for integrated technologies in support of road crack detection and determining its location.

1.4 Expected Outcome

Integrating the infrared thermography the global navigation system if successful, will create a reliable practical method in identifying the asphalt cracks and their locations.

Infrared thermography is a technique that relies on transforming the heat released from an object into a visible picture. When asphalt is heated by the infrared radiation from the sun, defective areas will heat at a different rate than the undamaged (healthy) asphalt. Using an infrared camera to capture images of such locations, the defective areas will be shown in a different color in contrast to the healthy one. The main advantage of the infrared cameras is that they do not rely on visible light to operate; hence they could be used day or night. IR cameras technology has improved in the past two decades and it is used now in many areas for diagnostic and evaluation such as medicine, agriculture, environment and building inspection among others.

The global navigation satellite systems (GNSS) are widely used in many aspects of our daily life. They are used in navigation (cars, boats, airplanes and persons), surveying, mapping and also in some construction applications such as bridge deflection monitoring (Roberts et al., 2004) and road compaction (oloufa 1997). Currently there are two GNSS systems: The global positioning system (GPS) possess by the USA and the Russian navigation system (GLONASS). A third navigation system (Galileo) owned by the European Union will join the global navigation

systems in a few years. This is expected to further improve the reliability and accuracy of the satellite navigation systems and widen its applications.

The GPS system is a navigation system owned by the US Department of Defense. It consists of 24 satellites orbiting the earth in 6 planes and transmitting radio signals on two different frequencies (L1 & L2). With at least four satellites in view, a GPS receiver anywhere on earth at any time can detect the incoming signals from these satellites and determine its own location in terms of latitude, longitude and elevation.

The GLONASS is a navigation system owned by the Russian Federation. It is similar to the GPS system regarding the satellite constellation, orbits and signal structure. It also uses 24 satellites but in 3 orbital planes. These satellites transmit the same radio coded signals as the GPS satellites but at different frequencies.

The accuracy level obtained from GPS and / or GLONASS systems varies from meters level to centimeters level depending on the receivers` capabilities and other non-receiver related sources such as number of satellites in view, satellites geometry, surroundings around the receiver. The receivers are categorized by their ability to detect signals from single or dual systems (GPS/ GLONASS) in single or dual frequencies (L1 & L2). They vary greatly according to their features in price from a couple of hundred to many thousands of US dollars. For this reason, the receiver selection is essential for each type of application to achieve the desired level of accuracy at a reasonable cost.

1.5 Format of Thesis

This thesis consists of five chapters as follows:

- Chapter 1 presents an introduction giving the reader an overview of the subject and justification of the study.
- Chapter 2 is a review of the previous work done on asphalt crack detection as well as a general idea about the infrared radiation and infrared camera technology. It also contains review on GPS and GLONASS and how they work.
- Chapter 3 is the methodology used with description of the instruments and the procedures done before and during the testing.
- Chapter 4 demonstrates the results and discusses the outcome.
- Chapter 5 offers summary, conclusions and recommendations for future use and / or research related to the subject

2. LITERATURE REVIEW

2.1 Background

Pavement distress assessment is an essential process in road maintenance and management. It can provide the DOT management with the necessary information about distresses types and locations facilitating priority establishment and resources allocation.

The evaluation of pavement condition can be divided into two different, but related, categories. The first is examining the road's surface and the second is to investigate the subsurface condition. The ideal scenario is to use a nondestructive test for pavement evaluation (to avoid traffic disruption). Nowadays, there are many technologies that have been introduced in this area.

2.1.1 Surface Examination

There are several types of distresses that may develop in asphalt road pavement surface such as cracks, rutting, bleeding, swell, slippage, lane/ shoulder drop-off, patch and utility cut and many others. The major form of distress is cracks. Cracks are discontinuities in the road surface that can take different shapes and sizes. The most conmen type is the fatigue crack, which appears as an alligator skin, and consists of small cracks connected to each others. Other major types are the block cracking which divide the pavement surface into nearly rectangular pieces and the longitudinal and traverse cracks that may occur parallel to the road centerline or perpendicular to the road surface (Huang, 1993).

The severity of cracks is classified by the AASHTO into three levels. Namely, level 1 are cracks ≤ 3 mm in width, level 2 are cracks between 3 and ≤ 6 mm in width and level 3 is for cracks greater than 6 mm in width.

Distresses in the asphalt road surface can occur due to various reasons. It might occur due to improper design assumptions, wrong construction methods or materials. In addition, any changes in the underlying layers such as sink holes or broken utilities pipe can start with a form of surface distresses.

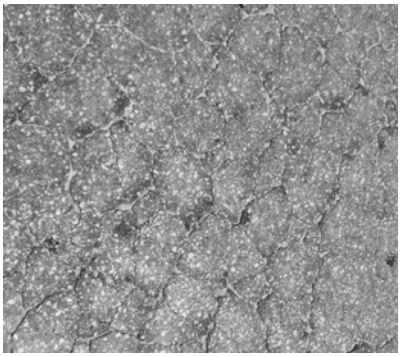

(a) Alligator Cracking

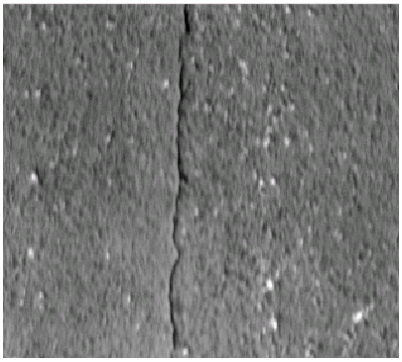

(b) Longitudinal Cracking

Figure 1 Different Types of Asphalt Cracks

2.1.2 Subsurface Investigation

Subsurface investigation is a helpful diagnostic tool. At times when the surface distress is severe, it could be used to confirm the cause of the distress and help in determining the maintenance method. The ground penetration radar (GPR) technology has proven to be a very powerful tool in this area. The GPR can detect the pavement and underlying materials' thickness, sub-grade compaction, utilities leakage, buried structures, material aging and many others. The GPR produces high frequency electromagnetic waves that travel through the layers of the ground

until they meet a target where they reflect to the surface. Changes in the material properties cause variations in the speed of the electromagnetic waves and its reflection where it could be sensed by an antenna at the surface of the earth and processed to produce a two-dimensional digital picture.

2.2 Methods of Crack Detection

Researchers have been trying to create new means for early, accurate, reliable and less expensive crack detection methods. The most commonly used method for crack detection is the visual method. This method was found to be extremely time-consuming, requires a lot of training, conveys safety hazards to the staff and is prone to errors. Hence, there is a need to develop an automated system for the accurate detection of cracks. This desired automated system should generally consist of an image capturing device, computer software to detect and analyze the distressed locations, and a positioning device that is able to tag the exact location of the distressed areas.

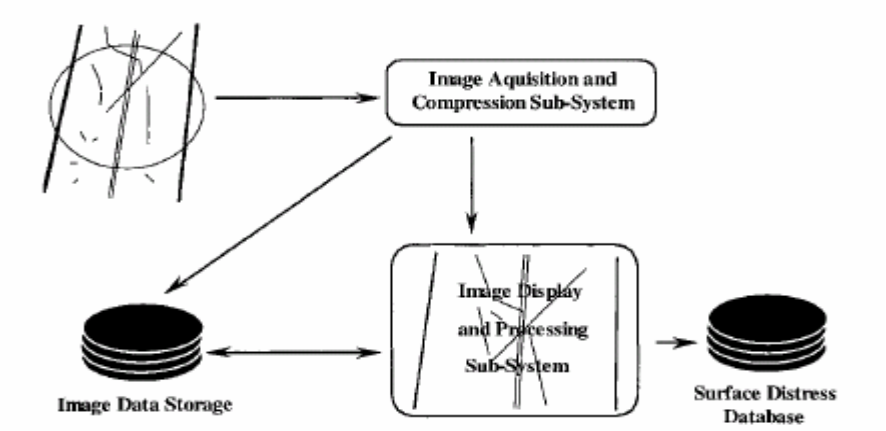

Figure 2: System Concepts in Pavement Surface Distress Survey
(Source: Wang, 2000)

Over the past two decades, several methods and equipment have been created to automate pavement surface distress detections. Wang (2000) studied the top six automated systems in terms of the image acquisition device and the image processing software used. These systems are

the Japanese Komatsu system, the US PCES system, the Swedish PAVUE system, the Swiss CREHOS, the Illinois Automated Road Inspection System, and the Canadian GIE System.

Some of the above mentioned systems utilize analog image acquisition devices. However, Wang (1999) described some problems with the use of analog-based cameras e.g. they do not give high resolution images (the maximum resolution is about 400 pixels per line), besides, the analog images needed to be digitized in order to be visualized by crack detection software.

Other automated systems utilize digital cameras for capturing images for the automated surface distress detection. There are two types of digital cameras, area-scan and line-scan. Line-scan cameras capture one strip of pixels at a time and so are considered to be one-dimensional. The area-scan cameras capture square images i.e. two dimensional. It was found that the line-scan cameras are better for capturing moving objects and for detection of small cracks up to a minimum width of 3.45mm (Gunaratne et al., 2004). The use of digital cameras allows the images to be processed directly by computers in real time and they yield higher resolution images than analog cameras.

In general, both digital and analog image acquisition cameras require ample amount of light to produce images with enough lucidity for the crack detection software to analyze e.g. Florida DOT has ten 150 watt lights each with polished reflectors mounted on the back of their data collection vehicle (Gunaratne et al., 2004) to produce enough light for the system to operate.

The most recent development in images acquisition for crack detection automated system is the use of infrared cameras. They have been primarily used in some construction areas such as bridge decks and roofing inspection applications. Recently, the infrared cameras were tested for detection of surface asphalt cracks against the conventional digital cameras. It was proven that

the infrared cameras generated images with excellent quality and reliability in the sun and shade even though their resolution was much less than the resolution of the digital cameras. This is mainly because the infrared cameras depend on changes in temperature and emissivity while the traditional imaging depends on changes in color (Oloufa et al., 2004).

2.3 Infrared Thermography

Radiation is a form of energy that travels and spreads out as it goes. Any object that has temperature greater than absolute zero K (or -273.15^{o} C) produces radiation. Objects radiate energy in the form of electromagnetic waves. The electromagnetic wave consists of electrical and magnetic fields. These fields are perpendicular to each other and to the direction of the wave. The electromagnetic spectrum is a name that scientists gave to a bunch of types of radiation. It can be described in terms of a stream of photons traveling in a wave-like pattern and moving at the speed of light. The difference between various types of electromagnetic radiation is the amount of the energy that exists in the photons. As shown in figure 2 for instance, the radio waves have photons with low energy; infrared has more, then visible light is next.

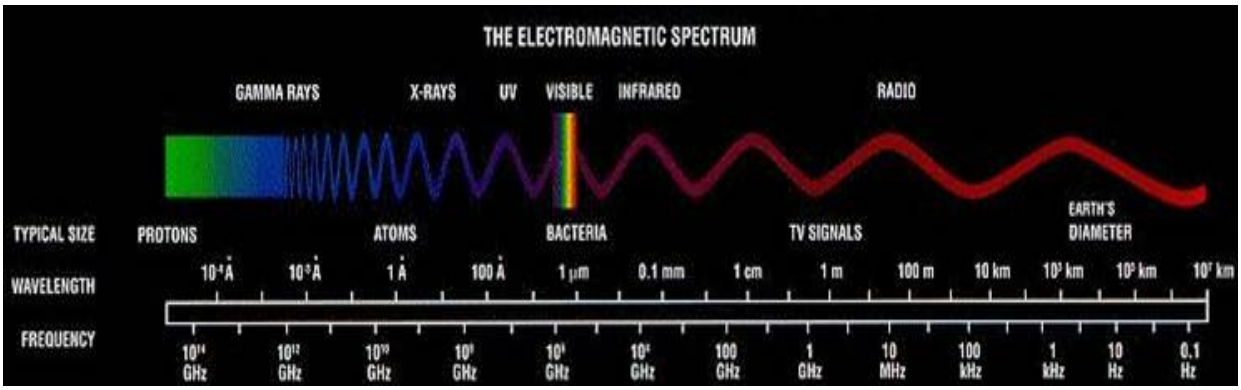

Figure 3: The Electromagnetic Spectrum
(Source: http://www.wel.atr.jp/ph/atrexpo/qd1.JPG)

The electromagnetic spectrum is arranged and divided into sections according to their frequency and wavelength. The frequency is the number of cycles per second and the wavelength is the distance from peak to peak. The frequency is proportional to the reciprocal of the

wavelength and is measured in hertz (Hz) while the wavelength is measured by the micron (one millionth of a meter). The shortest waves are gamma rays which have a wavelength of 10^{-6} microns and the longest is the radio waves which have a wavelength of many kilometers.

Visible light is a unique type of electromagnetic radiation that occupies a small portion of the electromagnetic spectrum. It is the only electromagnetic wave that can be seen by our naked eyes as the colors of rainbow. Each of these colors has a different wavelength and they have a range from 0.4 micron (violet) to 0.7 micron (red) of the electromagnetic spectrum. When an object does not have enough heat to radiate visible light, it emits most of its energy in the infrared range.

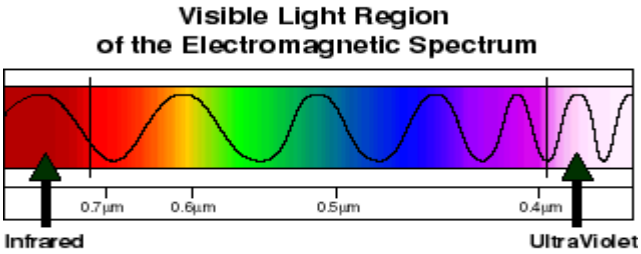

Figure 4: Visible Light Regions
(Source: http://imagers.gsfc.nasa.gov/ems/visible.html)

The infrared light falls between the visible light and microwave region at the electromagnetic spectrum. It can be divided into three different ranges of wavelengths. The near infrared lies between 1.0 to 3.0 µm, the far infrared is from 6 to 15 µm and the middle infrared in between the near and far.

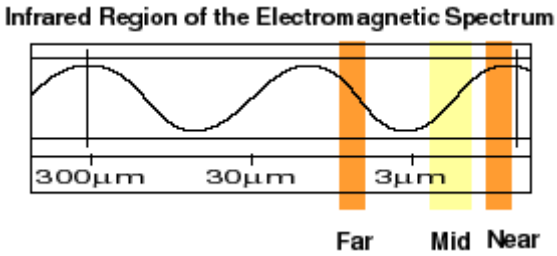

Figure 5: Infrared Region
(Source: http://imagers.gsfc.nasa.gov/ems/infrared.html)

Because heat is the main source of infrared radiation, any object that has a temperature radiates in the infrared. Heat can be transferred from an object to another as a result of temperature variation in different ways. On of these ways is radiation which refers to the transfer of energy from one object to another through electromagnetic radiation emitted by an object. The quantity of energy that leaves an object as radiant heat is proportional to its emissivity and its temperature. Emissivity is a material property, so any object has an emissivity value range from 1 for ideal emitter body (black body) to 0 (good reflector body).

2.3.1 Infrared Thermography Camera

Infrared thermography cameras produce images of invisible infrared radiation and can provide detailed temperature measurement (for the captured object) making it easy to identify and evaluate the areas of discrepancies. The sensor inside the IR camera absorbs the IR energy from the surface that need to be inspected, and converts it into electrical voltage to create the thermal images. It gives each temperature a different color or a gray level. IR cameras are categories as far or near cameras depending on the area (IR wave length) the sensor could operate. The IR cameras technology has been improved over the years, and they are now more durable and portable.

2.4 Global Navigation Satellite System

The global navigation system (GNSS) consists of satellites orbiting the earth and transmitting radio signals that are used by receivers to determine their geographic location. There are two GNSS systems functioning now, the global positioning system (GPS) and the Russian federation navigation system (GLONASS). By the year 2008, a third system owned by the European Union will be completed and ready for use. This will increase the integrity and the accuracy of navigation satellites systems.

2.4.1 The Global Positioning System (GPS)

The global positioning system (GPS) is one of the breakthroughs of the twentieth century. It was invented by the United States Department of Defense in the late seventies and was fully completed by the year 1993. The system was mainly built for military purposes such as weapon guidance and military navigation. It also has civilian applications, with a lesser accuracy. Over the years, it gained an important role, and it is used now for many applications; for example surveying, mapping, vehicle navigation, and construction.

2.4.1.1 System Overview

The GPS system consists primarily of three segments:

1. *The space segment*: consists of at least 24 satellites orbiting the earth in six orbital planes where 4 satellites exist in each plane. The orbits are inclined 55 degrees in respect to the equator, spaced 60 degrees around the equator and about 12,000 miles away from the earth surface. The satellites vehicles (SV) are traveling at 7,000 miles per hour, thus they

complete one round around the earth in 11 hours, 58 minutes. The satellite vehicles are powered by solar energy and they have backup batteries to be used in case of solar energy fails. Each of these satellites transmits radio signals. With such arrangement, any GPS user can be able to detect signals from at least four satellites any time of the day and anywhere on the globe.

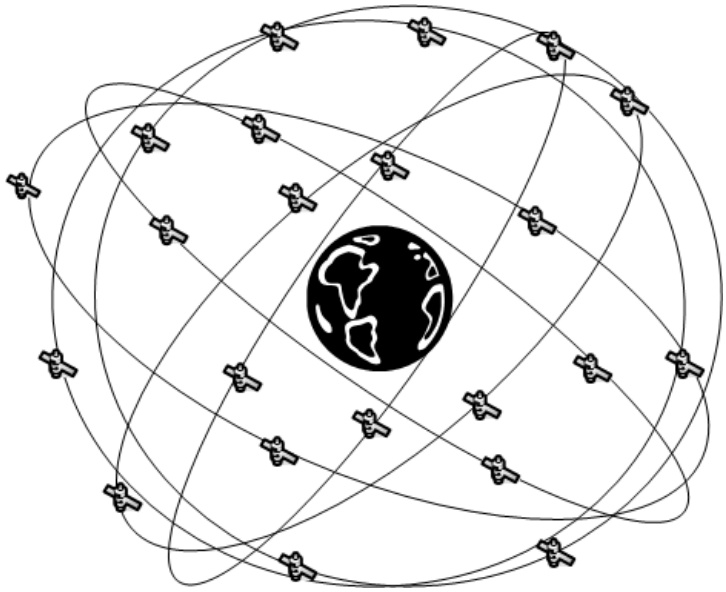

Figure 6 Satellites Constellation

2. *The control segment*: the purpose of this segment is to observe the health and condition of the satellite vehicles and to provide them with orbital and time corrections. It consists of a worldwide network of tracking stations including four monitor stations, four ground antennas, and a master control station located at Colorado Springs, Colorado.
3. *The user segment*: consists of the receiver and antenna operated by any user anywhere on the earth. These receivers are capable of receiving radio signals from the satellites and

calculating the user's longitude, altitude and latitude to determine the user's location on earth.

2.4.1.2 The GPS Signals

The GPS satellites transmit low power radio signals on two carrier frequencies, L1 at frequency of 1575.42 MHz and L2 at frequency of 1227.60 MHz. The satellites transmit the navigation data and Pseudo-Random codes on these two carrier frequencies. The navigation messages contain the information that depicts the system status e.g. GPS satellite orbits and clock corrections. The Pseudo-Random codes are a complex pattern of digital codes. There are two different types of Pseudo-Random codes, C/A code and P- code.

2.4.1.2.1 Course Acquisition (C/A-code):

It is a repeating pseudo-random noise (PRN) in a way that it produces random noise like codes that could be exactly repeated. Each satellite has its own PRN code so that it is used as an identification number for the GPS satellites. C/A-code is sent on the L1 band only and is referred to as "Standard Positioning Service" (SPS). It is easy to jam and spoof C/A code decreasing its accuracy.

2.4.1.2.2 Precision code (P-code)

P-code provides highly precise location information. The U.S. military is the primary user of P-code transmissions and it can be encrypted. When it is encrypted it is called Y-code. In this case, only special receivers can access the information in order to prevent unauthorized access. The P-code signal is broadcasted on both L1 and L2 bands. P-code broadcasts are known as "Precise Positioning Service" (PPS).

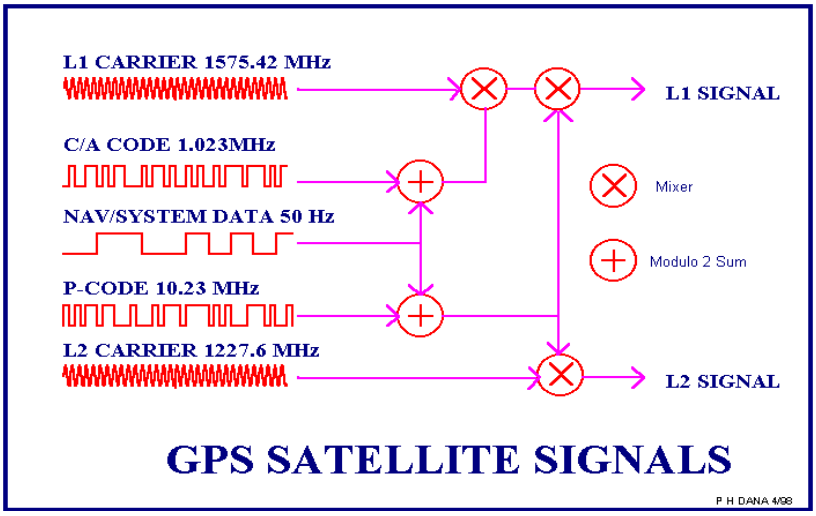

Figure 7 : GPS Satellite Signal Structure
(Source: P N Danna 1998)

2.4.1.3 How Does the GPS System Work?

The theory for operating the GPS is based on the well known equation:

Distance = Time x Speed. *(2.1)*

Therefore, by knowing the time the signal spent to travel form the satellite until it reaches the receiver, and by knowing the speed of light (186,000 mile/sec) the receiver is able to calculate the distance between his antenna and the satellite. That defines a surface of sphere of possible receiver locations. By knowing the distance to another satellite, there will be an imaginary two spheres intersecting in a circle of possible locations. A third distance to a satellite will give us a third sphere that intersects with the circle in two points. One of these points will be the location of the receiver antenna and the second will not be a possible solution (e.g. position is out side the earth), so it will not be considered. Although theoretically three satellites in view are enough to determine the receiver position, a fourth satellite is needed to get over the receiver clock error by synchronizing it with the atomic clock on board the satellite (Hun, 1993).

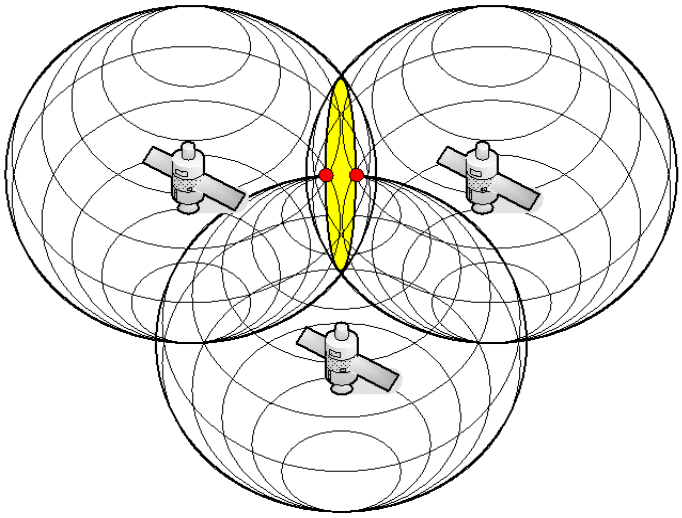

Figure 8 GPS Position Determination

2.4.1.4 GPS Accuracy and Error Sources

The accuracy of GPS can be described as the degree of conformance between the measured velocity, position and time of a GPS receiver and its actual velocity, time and position as compared with a constant standard (Fundamentals of GPS, 1996). The GPS system accuracy is affected by several types of errors. These errors could be categorized into three main groups: those created at the satellites, the receiver, and the atmosphere. In addition to that, the number of satellites in view and the satellites geometry has considerable effect on GPS accuracy.

2.4.1.4.1 Selective Availability:

This is an artificial error implemented by the U.S. Department of Defense for national security. It was generated because it was found that the accuracy obtained using the civilian C/A mode receivers is the same as that obtained from the military p-code receivers. It gives a 30 meter range error that varies over time. This error was discontinued on May 2000.

2.4.1.4.2 Satellite Clock Errors

Each satellite has and on-board atomic clock. Although these clocks are highly accurate, they are not perfect. They give an error of about 8.64 to 17.28 ns per day which yields a range error of about 2.59 to 5.18 m (El-Rabbany2002).

2.4.1.4.3 Ephemeris Errors

It is also known as orbital errors; these are inaccuracies of the satellite's reported location.

2.4.1.4.4 Receiver Clock Error

This error affects all measures from the receivers to all the satellites by the same amount. It could be avoided by performing simultaneous measurements from at least four satellites. The receiver then can detect the error and apply the correction to all measurements from that moment on.

2.4.1.4.5 Multi-path Error

This is a major error source. It occurs when the receiver antenna gets two or more signals at different times from the same satellite instead of one. This is due to the reflection of signals on various surfaces surrounding the receiver antenna which leads to strengthening of the signals. This error was reduced over time with the application of new technologies in receivers.

2.4.1.4.6 Receiver Measurement Noise

A good GPS system should have a minimum noise level. This noise results from the limitations of the receiver's electronics.

2.4.1.4.7 Ionospheric Delay

The ionosphere is the band of the atmosphere form around 50 to 1000 km above the surface of the earth. The ultraviolet and X- ray radiation from the sun interact with gas molecules in this band resulting in free electron being released from the atoms and yielding large number of free negatively charged electrons and positively charged atoms. This is called gas ionization. When the electromagnetic GPS signals are propagated through this medium dispersion occurs, changing the velocity of the propagated signal. The ionospheric propagation delay will cause the measured range to be longer than the true range.

2.4.1.4.8 Tropospheric Error

The troposphere is the band that surrounds the earth and extends to about 50 km from the surface of the earth. Although it is full of water vapor and varies in temperature and pressure, it causes relatively little error. Both the ionospheric and tropospheric errors can be minimized by using mathematical modeling. It is done by predicting the amount of delay that can be introduced to the signals by traveling through the atmosphere during day and night.

2.4.1.4.9 Satellite Geometry Error

The satellite geometry represents the geometric location of the GPS satellites as seen by the receiver. The more spread out the satellites are in the sky, the better the satellite geometry and vice versa. The error of the satellites geometry can be measured by a number called the Dilution of Precision (DOP). Lower number of DOP means good satellite geometry and less error.

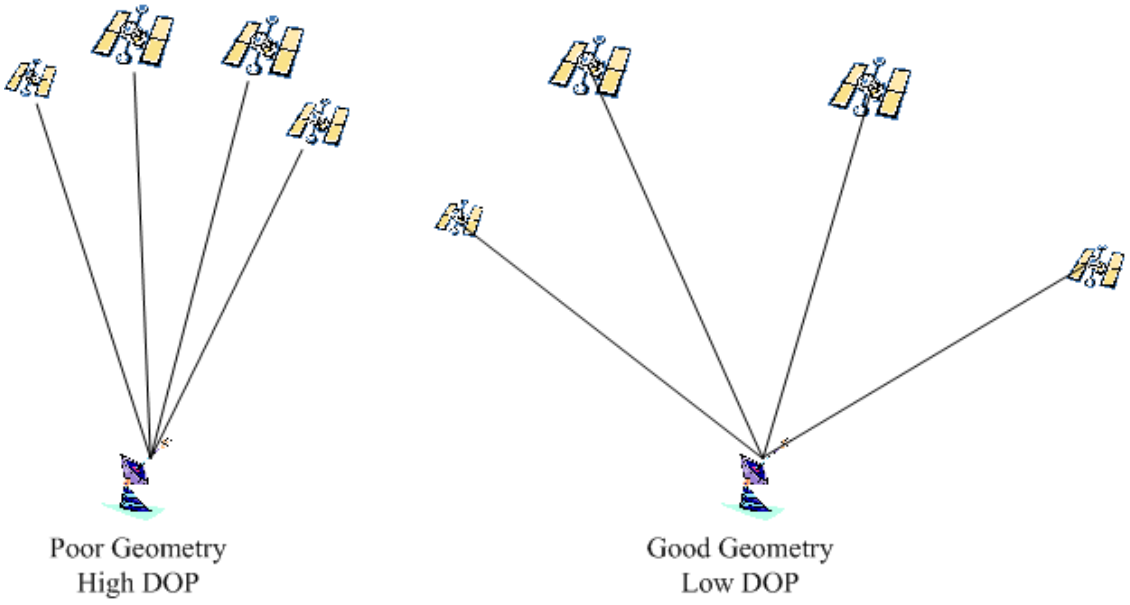

Figure 9 Poor and Good Satellite Geometry

Table 1 shows a list of errors sources and its impact on the GPS data obtained in SPS measurements.

Table 1: Expected GPS Errors in SPS Measures

Error Source	**Standard GPS (m)**
Satellite Clocks	1.5
Ephemeris	2.5
Ionosphere	5.0
Troposphere	0.5
Receiver Noise	0.3
Multipath	0.6
Selective Availability	30.0

(Source: GPS Fundamentals & Applications 1996)

2.4.1.5 GPS Positioning Types

2.4.1.5.1 Stand- alone Position

This type of position acquisition uses a C/A code (or P code for authorized users) and requires only a single receiver. The accuracy of such system ranges between 15-100 meters. The position is subject to all types of errors. It is suitable for all application that doesn't require a high degree of accuracy e.g. car or boat navigation.

2.4.1.5.2 Differential GPS Position

The differential GPS (DGPS) is an advanced technique that is used to obtain more a precise position from a GPS receiver. It involves at least two receivers. One is stationary at a known location called the "base receiver". The other(s) receiver moving or standing at the unknown locations and it is known as the 'rover receiver". Both receivers should be acquiring signals from the same satellites, so there is a limitation to the distance between the base and the rover. The base receiver does backward calculations as it uses its known location to calculate the time that a signal from a certain satellite should take to reach the base receiver. Then it compares it with the actual time the signal spent traveling from the satellite to the receiver. The difference will be the error correction factor. The base receiver then transmits this error information to the rover receiver (through internal modem radio) so it can use it to correct its measurements. The accuracy obtained by DGPS method can vary from couple of meters to sub-centimeters depending on the receivers capabilities and type of GPS measurement utilized (Abousalem, 1996). The sub-centimeters accuracy level can be achieved by using the RTK technique.

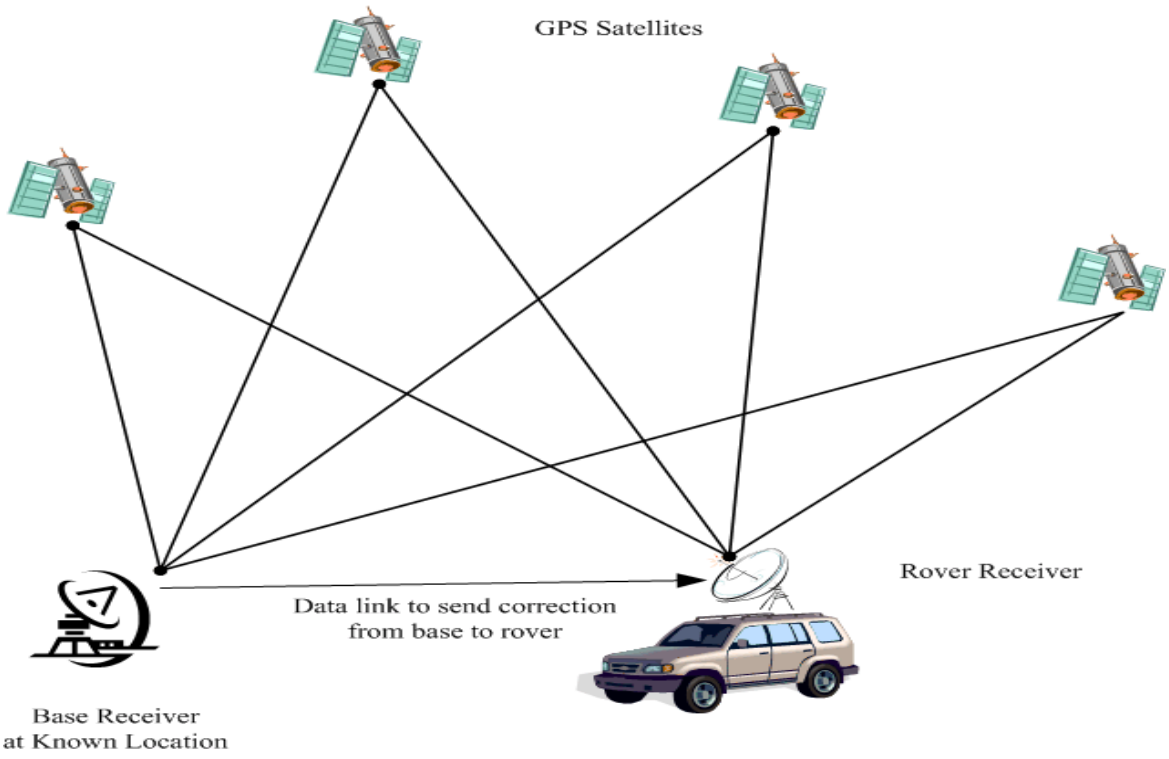

Figure 10 DGPS Technique

2.4.1.5.3 Real-Time Kinematic (RTK)

The real-time kinematic is a technique that is uses both the coded signals (C/A code or P-code) and the carrier phase (L1 and L2) in determining locations. The software inside the receiver, calculates the integer numbers of carrier phase wavelengths between satellites and GPS receiver antenna. This process called “initialization” and is known also as fixing the integer or resolving ambiguity. During the initialization time the receiver is in RTK float solution and once the integer is fixed the receiver gets the RTK fixed status. The RTK fixed solution is the highest level of accuracy that can be ever achieved by DGPS.

The time that the receiver will take to fix the integer varies from a few seconds to several minutes according to receiver capability (single or dual frequency/system), the number of satellites in view and the strength of the multipath signals (www.javad.com).

The RTK fixed solution requires more than four satellites in view and the accuracy level could drop anytime to RTK float if there are not enough satellites to track or an existence of any obstacles around the receiver's antenna. Table 2 Shows the expected accuracy obtained from different methods of using GPS.

Table 2: Expected Accuracies in Different Measuring Techniques

Autonomous (Stand Alone)	Accuracy	15 - 100 meters
Differential GPS (DGPS)	Accuracy	0.5 - 5 meters
Real-Time Kinematic Float (RTK Float)	Accuracy	20cm - 1 meter
Real-Time Kinematic Fixed (RTK Fixed)	Accuracy	1cm - 5 cm

(Source: http://www.gisdevelopment.net/tutorials/tuman004pf.htm)

2.4.2 The Russian Navigation System (GLONASS)

The Russian navigation system (GLONASS) is similar to the GPS. It consists of 24 satellites orbiting the earth in three orbits. The orbits are nearly circular and are 19,100 km from the surface of the earth. The orbits are inclined 64.8 degrees to the equator and the orbital time is 11 hours and 15 minutes. The satellites broadcast the same coded signals (C/A and P-code) on the two carrier waves (L1 & L2) exactly as in GPS. The only difference is that the carrier waves have different frequencies.

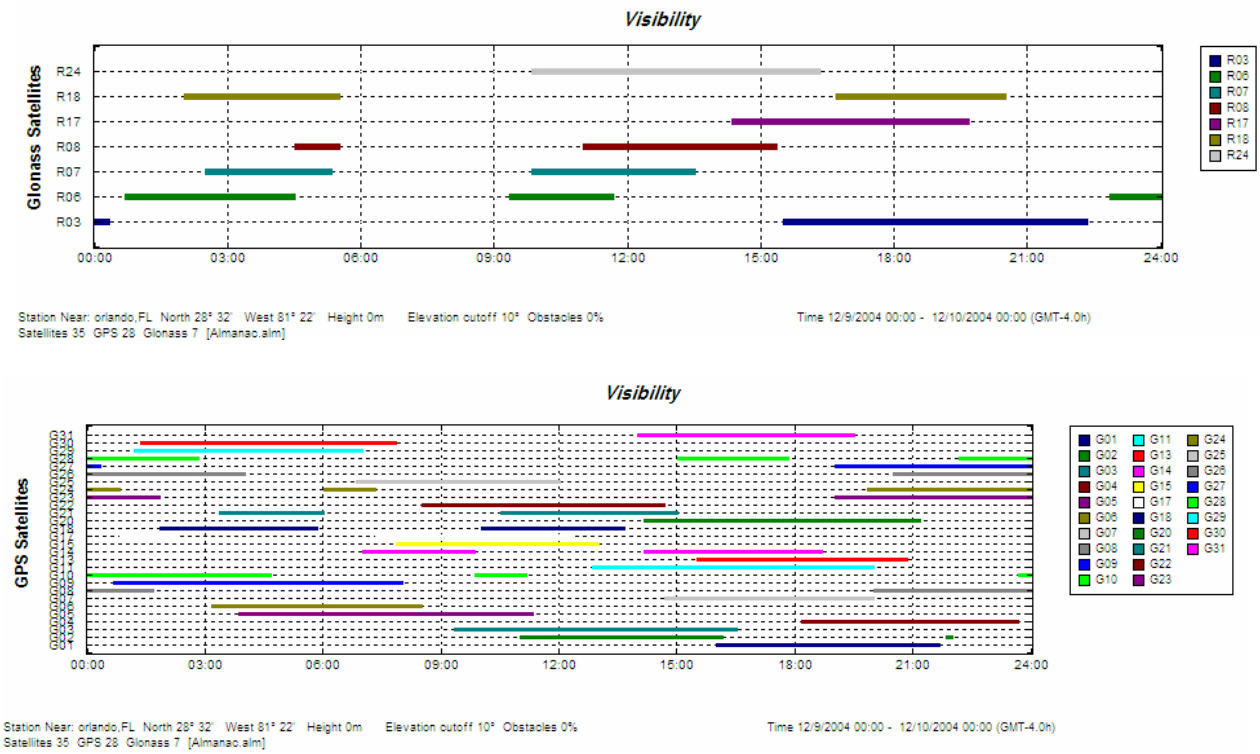

Figure 11: Comparison between Number of Satellites in View over Orlando in 24 Hours for GLONASS and GPS Systems

(Source: Trimble Navigation Planning)

2.5 The Proposed Integrated System

The proposed integrated system consists of an infrared camera mounted on a vehicle and facing downward to capture real time videos of the road surface. A GPS antenna is mounted on the vehicle as well for determining of the images' locations. Both the infrared camera and the GPS receiver are connected to a device that overlays the GPS coordinates on the images captured by the camera. The images could then be stored on the hard disc of a laptop or video tapes to be processed offline using crack detection software. The final images are expected to show the picture of the road surface with the detected cracks laid on top of it as well as its location in terms of longitude and latitude. Figure 12 shows a schematic diagram of the proposed system.

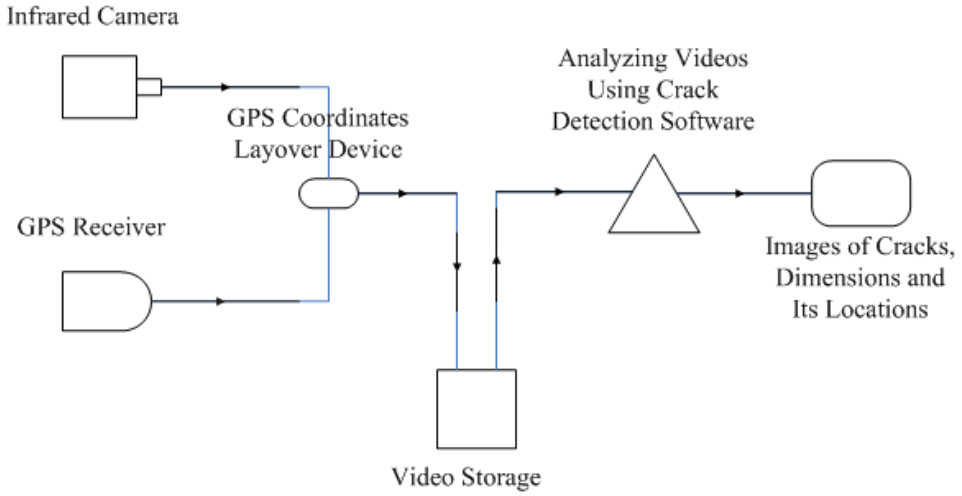

Figure 12 Proposed Crack Detection Integrated System

An example for the output of the GPS overlay devices can be seen in Figure 13. The location (longitude and latitude) coordinates are shown in the upper left side. Other information can be also seen such as vehicle speed, temperature, date and time.

Figure 13 GeoStamp™ Output Showing a Capture Image and its Location
(Source: http://www.icircuits.com/prod_geostamp.html)

3. EXPERIMENTAL WORK

To achieve the of research objectives, two separate tests were conducted. One to obtain the GPS/ GLONASS accuracy using DGPS technique and to select the most economic receiver parameters needed. The other was to evaluate the images taken by an infrared camera moving at different speeds, capturing images of the asphalt road surface using crack detection software. Both tests procedures and the tools that were used are described in detail below.

3.1 The GPS / GLONASS Test

Data acquisition was performed using two pairs of GPS receivers equipped with internal radios modem, external GPS antenna and radio antennae, all manufactured by Javad Navigation. One of the receivers was used as a base (fixed location) and the other was used as a rover. These receivers were selected for this research because they are able to detect dual systems (GPS and GLONASS) satellites` signals in single and dual frequencies (L1- L2) and they can operate in DGPS - RTK mode.

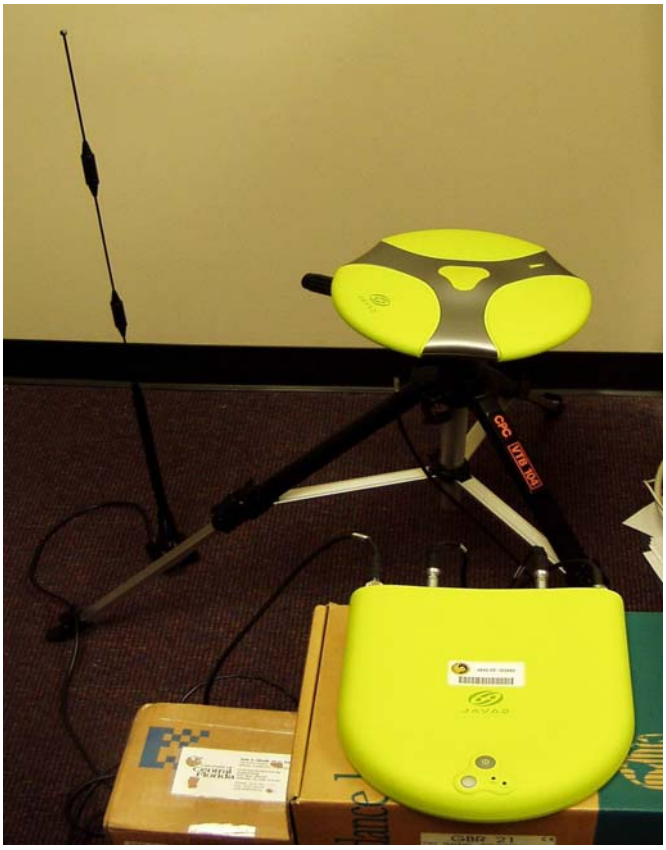

Figure 14: The Javad Legacy Receiver and Antennae

3.1.1 Base Receiver Settings

The base Station (GPS receiver) was installed in the mechanical room at the UCF engineering building I. The GPS and radio antennae were mounted on top of the same building and connected to the base receiver. The receiver was connected to a permanent power source inside the mechanical room. The base parameters were set to acquire signals from both systems (GPS and GLONASS) in dual frequencies (L1 and L2) and the RTK mode was enabled. It was also set to send DGPS corrections to the rover receiver. These settings were made by means of a laptop connected to the receiver through the serial port and with the use of PCView software. The parameters were fixed during the whole experimental period.

Figure 15: GPS and Radio Antennae for the Base Receiver

3.1.2 Rover Receiver Settings

The rover receiver and antennae were used by the researcher in collecting data from a location that is about 500 ft from the base receiver. The rover was connected to a laptop through the serial port and the PCView software was used to change the receiver parameter and to view the location's geodetic coordinates. Different settings were applied to the rover as follows:

1. Single frequency (CA/Code only) with the GPS mode.
2. Single frequency (CA/Code + L1 carrier phase) with the GPS mode.
3. Dual frequency (C/A Code + L1 and L2 Carrier Phase) with the GPS mode.
4. Single frequency (CA/Code + L1 carrier phase) with the GPS and GLONASS modes.
5. Dual frequency (C/A Code + L1 and L2 Carrier Phase) with the GPS and GLONASS modes.

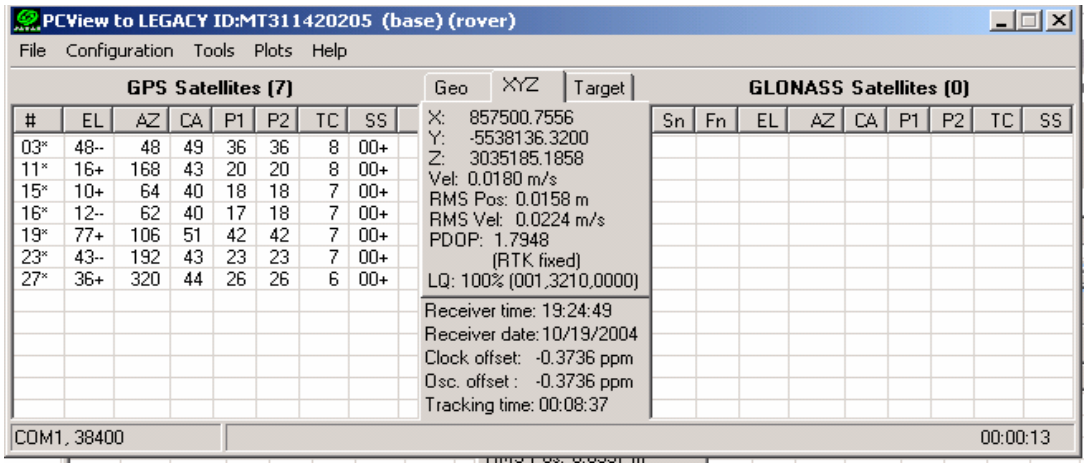

Figure 16: The PCView Software Screen

Each of the above parameters was set to the rover for a period of 2 - 3 hours. During this time, video clips for the PCView screen were recorded by Snagit 7 software, showing the geodetic coordinates for the point being monitored. The choice of Snagit 7 was made to overcome the lack of the receiver's internal memory. The recorded clips were saved to the laptop hard disc and were tabulated later on for each setting using Microsoft Excel.

3.1.3 Data Analysis

The geodetic coordinates obtained from the site were tabulated for each setting and an average reading for the X and Y coordinates was calculated. The variation between each reading and the average value was obtained and a graph was drawn to show the mean (X, Y) with all the other readings scattered around it.

To show and compare the different modes, the distance root mean square was calculated (the distance from a reading to the average reading) for each setting. The Cumulative frequency was then computed and another graph was drawn representing the percentage of the sample in relation to the distance from the mean (the presumed location).

3.2 Cracks Detection and Images Processing Test

3.2.1 Equipment Used

1. Infrared camera: the IR camera that was used for this test is Merlin® MID from FLIR system. The Merlin MID has spectral range from 1 - 5 μ m and has a 320 x 256 FPA for high resolution images. The IR camera has also variable integration time (from 5 μs – 16.5 ms) to avoid image saturation. The camera interface has a connector to PC and another connector to video recorder. So the output clips can be recorded on a PC hard disk and /or video tapes.(http://www.flirthermography.com/cameras/camera/1065/)

Figure 17: Merlin® IR Camera
(Source: http://www.flirthermography.com/cameras/camera/1065/)

2. ThermaCam researcher software: the main purpose for using this program is to deal with the live IR images that arrive to the laptop through the connection with the IR camera and to set IR camera to record images (or to stop) of the desired locations. It could also be used to show IR images, record them on a disk and analyze them later.

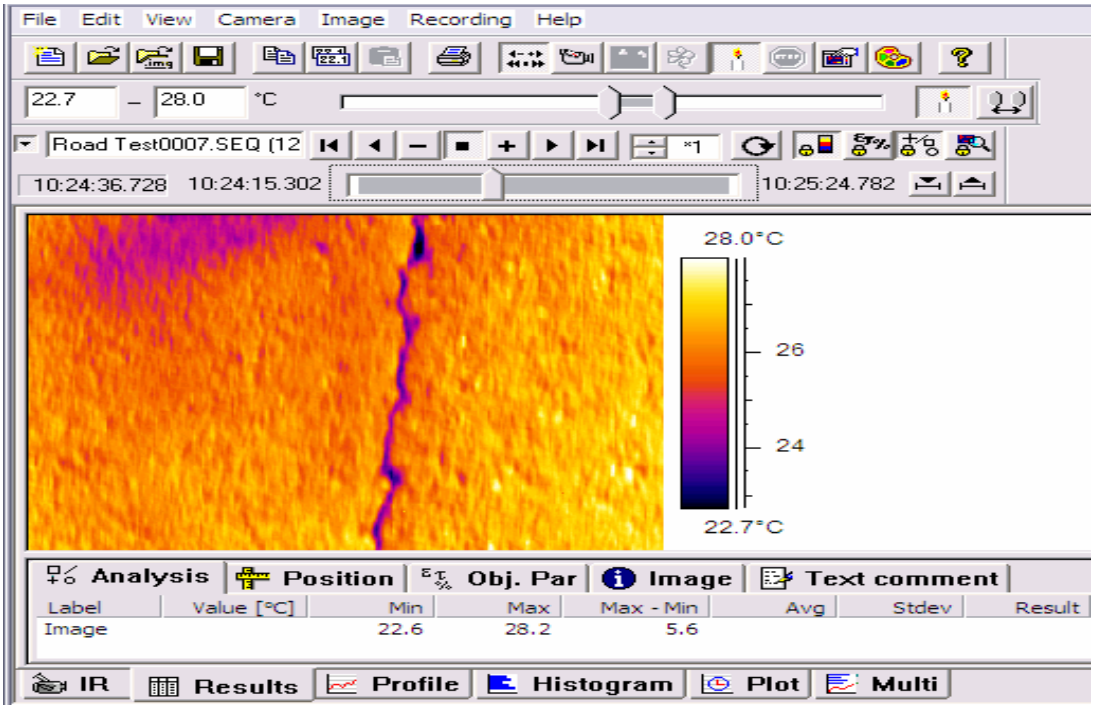

Figure 18: Thermacam Researcher Software Screen

3. WiseCrax® software: This is an automated cracks detection program developed by Roadware. It can acquire images automatically from videotape and detect, analyze and classify cracks up to 3 mm (Roadware, 2004).The result can be modified manually for quality control purposes.

3.2.2 Test Procedures

1. The IR camera was mounted and securely fixed to the back of a vehicle. The distance from the camera lens to the ground surface was 4 feet and the used lens was 25 mm. With such arrangement, the image from IR camera represents 480 mm x 310 mm of the asphalt surface. The IR camera was connected to a laptop inside the vehicle that has ThermaCam

research program installed. A videocassette recorder (VCR) was also connected to the infrared camera to record video clips of the road surface during the test.

Figure 19: IR Camera mounted at the Vehicle

2. The test was conducted in Tampa suburbs. The IR integration time was set to 1700 μm. and the vehicle moved at speeds 20, 30, 40, 50 and 60 mph. At each speed, video clips were taken by the IR camera to the road surface. Then the integration time was reduced to 500 μm and new pictures were taken at the different speeds.
3. A number of images from each group of video clips were selected using the ThermaCam researcher software in bmp format. The images were then converted to Jpeg grayscale 8

bits per pixel using InfraView software and the comment field was filled with information about the resolution and the size that one pixel represents in reality.

4. The image was processed by WiseCrax® for the detection of cracks and to determine the quality of the pictures in relation to the different speeds. The output of the images has the detected cracks marked on top of it and a statistical table attached to it showing cracks length, width and other information.

4. MAJOR FINDINGS

The results are presented in two sections. The first section shows the results from the GPS/ GLONASS test and the second presents the analysis of the processed images taken during the infrared camera test

4.1 GPS Test Results

Figures 20 to 25 show the results from the GPS tracking test in each different mode. The intersection of the Y axis and X axis represents the average reading. The entire readings are shown scattered around the average reading. Figure 20 shows the rover readings in C/A mode only. About 95% of the readings are within 158 cm from the origin. This is a higher accuracy value than we may expect (usually it is from 50 – 500 cm). This may be attributed to the base settings which was set to receive both GPS / GLONAS and in dual frequencies.

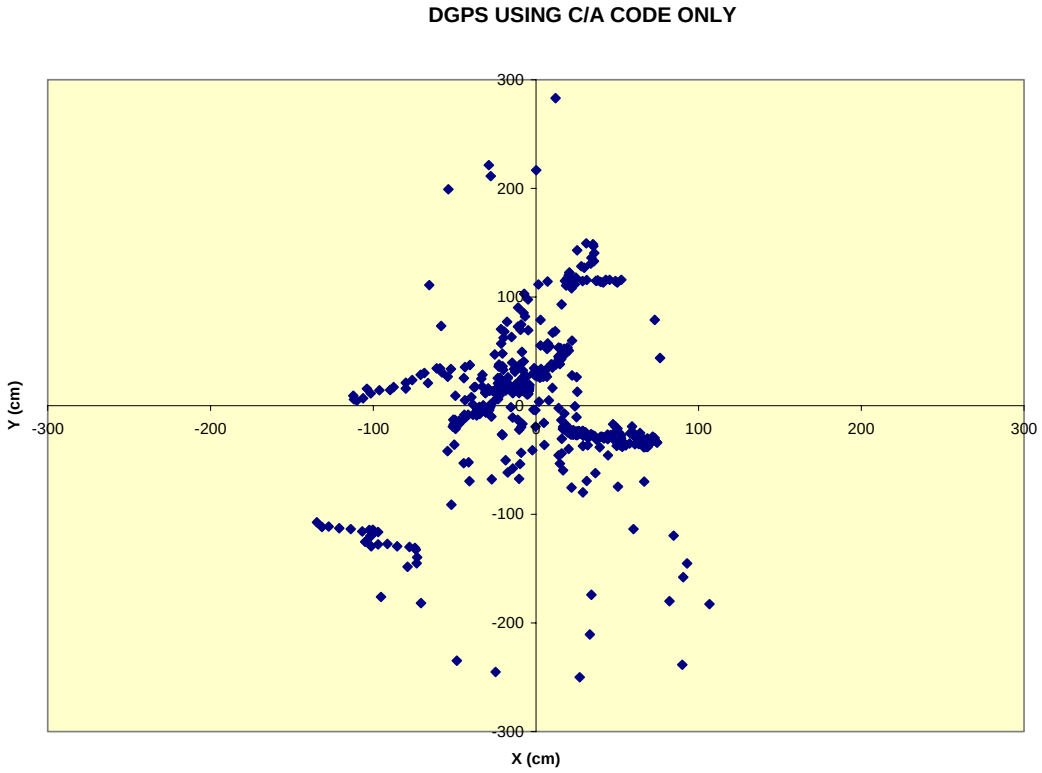

Figure 20: Location Based on C/A Code Only

Figure 21 shows the results from the rover receiver in a GPS only single frequency L1 and in float status. The graph shows that 95% of the readings are within 120 cm away from the origin.

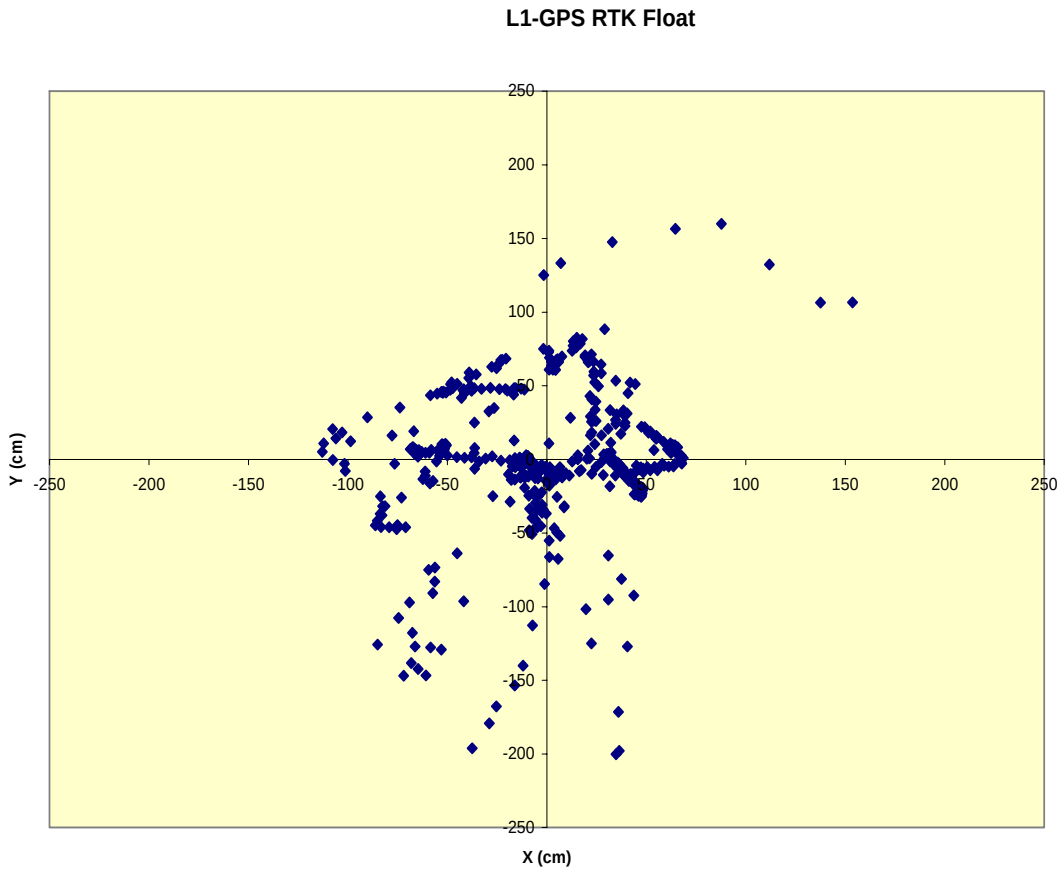

Figure 21: Location Based on L1-GPS RTK Float

Figure 22 illustrates the readings from the rover receiver in dual system GPS / GLONASS and in single frequency. It shows that 95 % of the readings are at nearly within 120 cm from the origin.

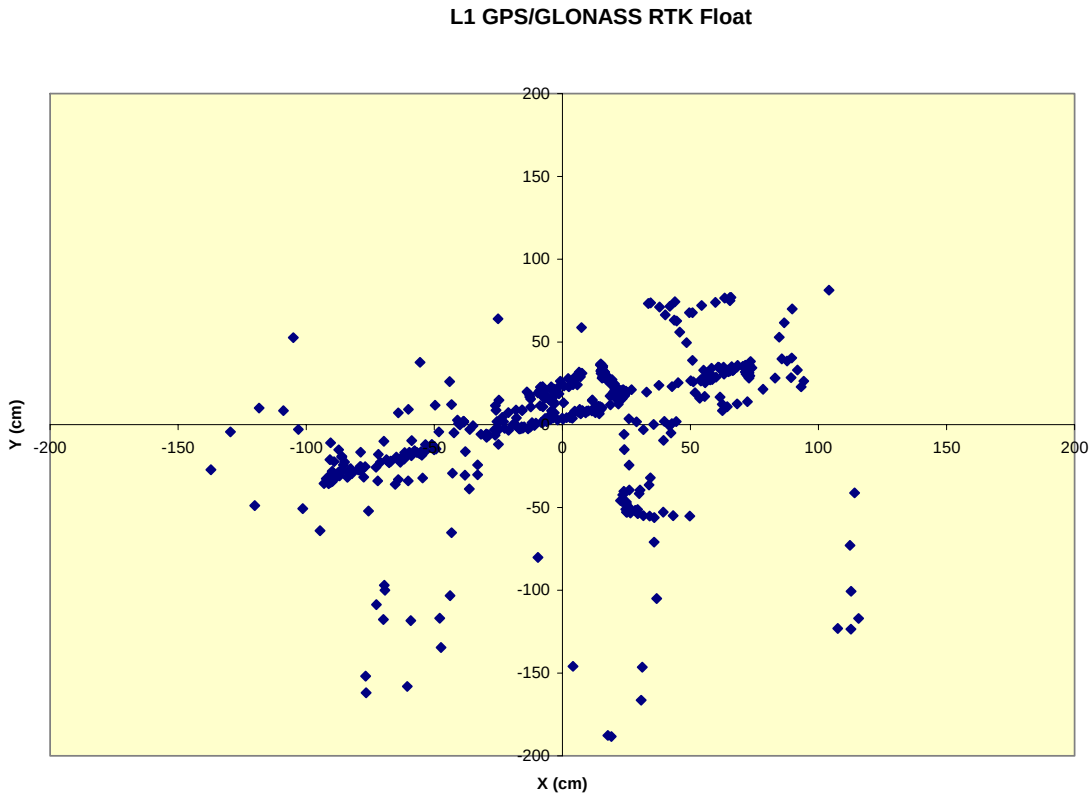

Figure 22: Location Based on L1 GPS/GLONASS RTK Float

Figure 23 demonstrates the readings from the rover receiver in GPS only single frequency L1 RTK fixed mode. The receiver didn't maintain RTK fixed solution for a long time and it always dropped back to RTK float mode. As shown in the graph, 95 % of the readings were within 7.5 cm only from the origin.

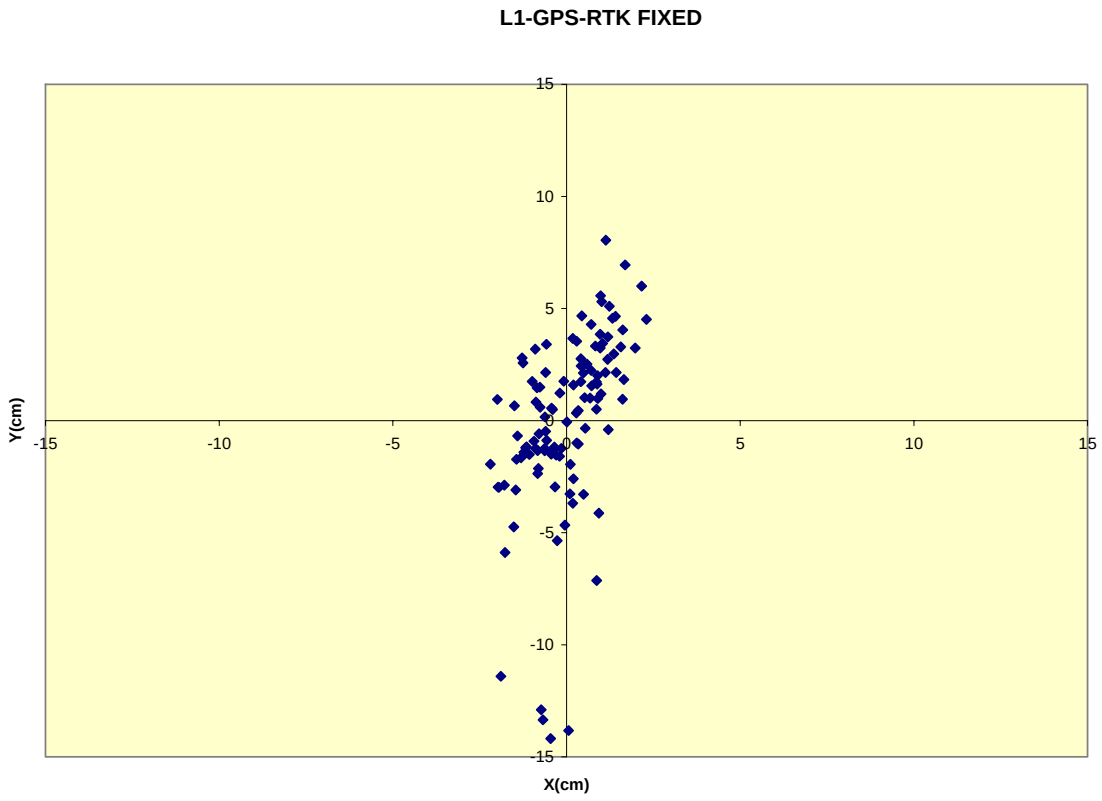

Figure 23: Location Based on L1 GPS RTK Fixed

Figure 24 shows the result from the test when the rover receiver was set to dual system GPS/ GLONASS, in single frequency (L1) and in RTK fixed mode. It shows that 95% of the readings were within 5 cm from the origin. It is within the expected range and the receiver maintains the RTK fixed solution all the times during the test.

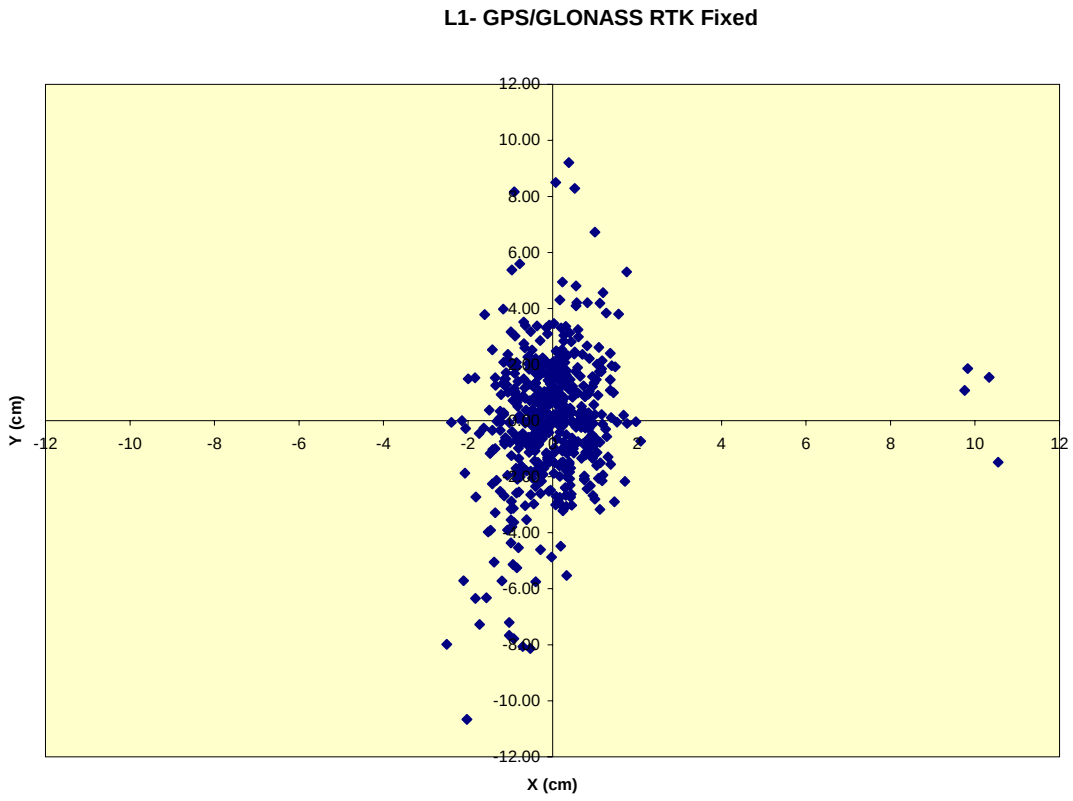

Figure 24: Location Based on L1 GPS/GLONASS RTK Fixed

Figure 25 shows the reading from the receiver when it was set to single system GPS and dual frequencies L1 and L2. The graph shows that 95% of the readings are within 5 cm from the datum.

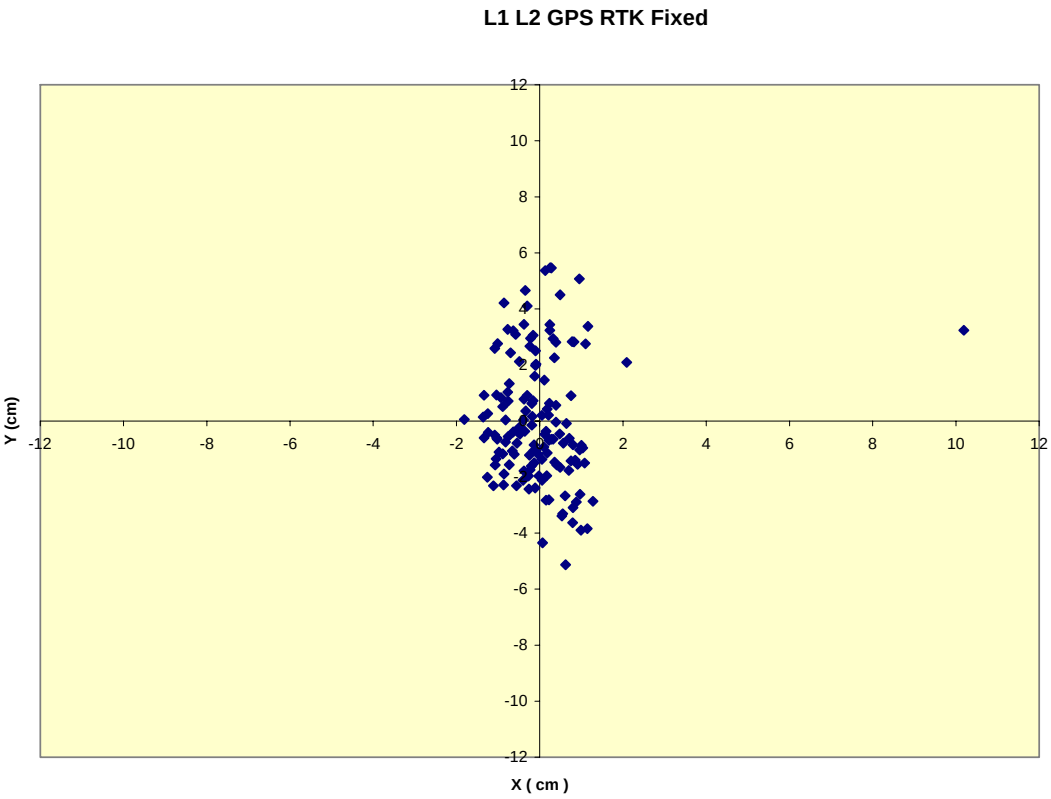

Figure 25: Location Based on L1-L2 GPS RTK Fixed

Figure 26 shows the reading from the receiver when it was set to dual system GPS/ GLONASS and dual frequencies L1 and L2. The graph shows that 95% of the readings are within 4.5 cm from the datum.

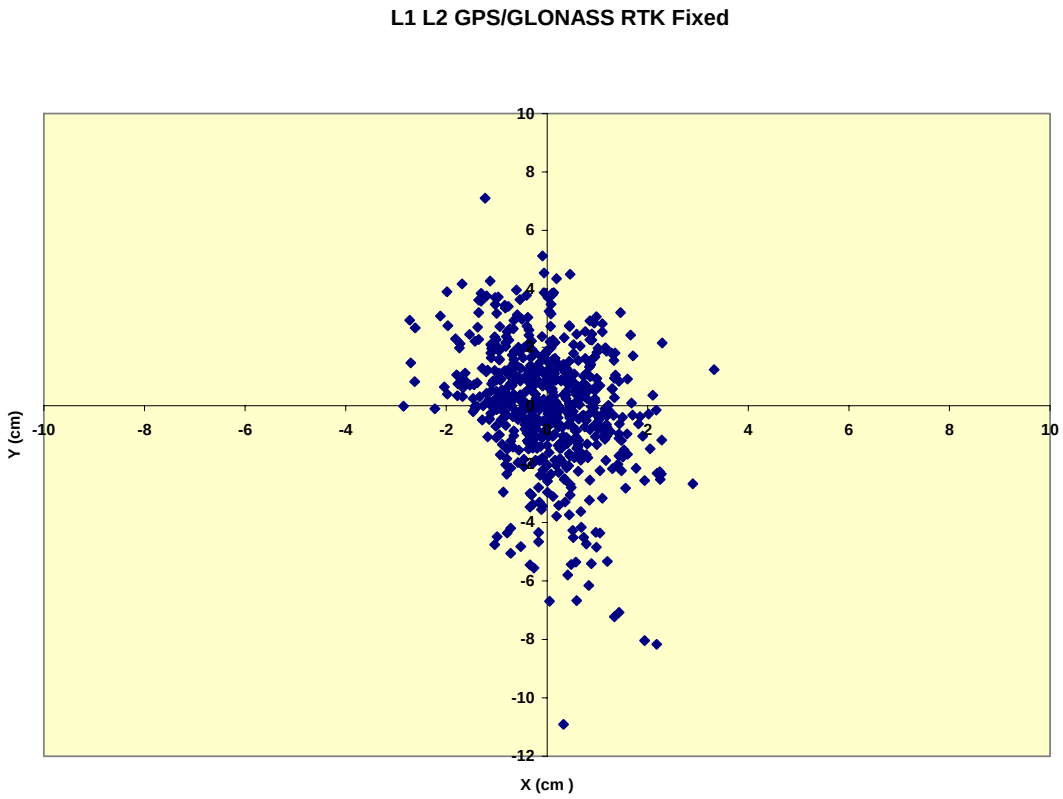

Figure 26 L1 & L2 in Dual Systems GPS/ GLONASS RTK Fixed

Figures from 27 to 30 are a comparison between the test results form different modes. They provide a clearer view for receiver parameters selection.

In figure 27, a comparison was made between the use of C/A code only and the use of RTK float solutions in GPS only and in GPS / GLONASS modes. It showed that C/A code achieved better accuracy than GPS and GPS/ GLONASS RTK float in some areas of the curve. This is not logical but it could happen due to external factors such as the number of satellites in view or the geometry of the satellites (DOP) or the surroundings around the receiver antenna. This proves that the position accuracy depends not only on the receiver parameters, but also on other external factors.

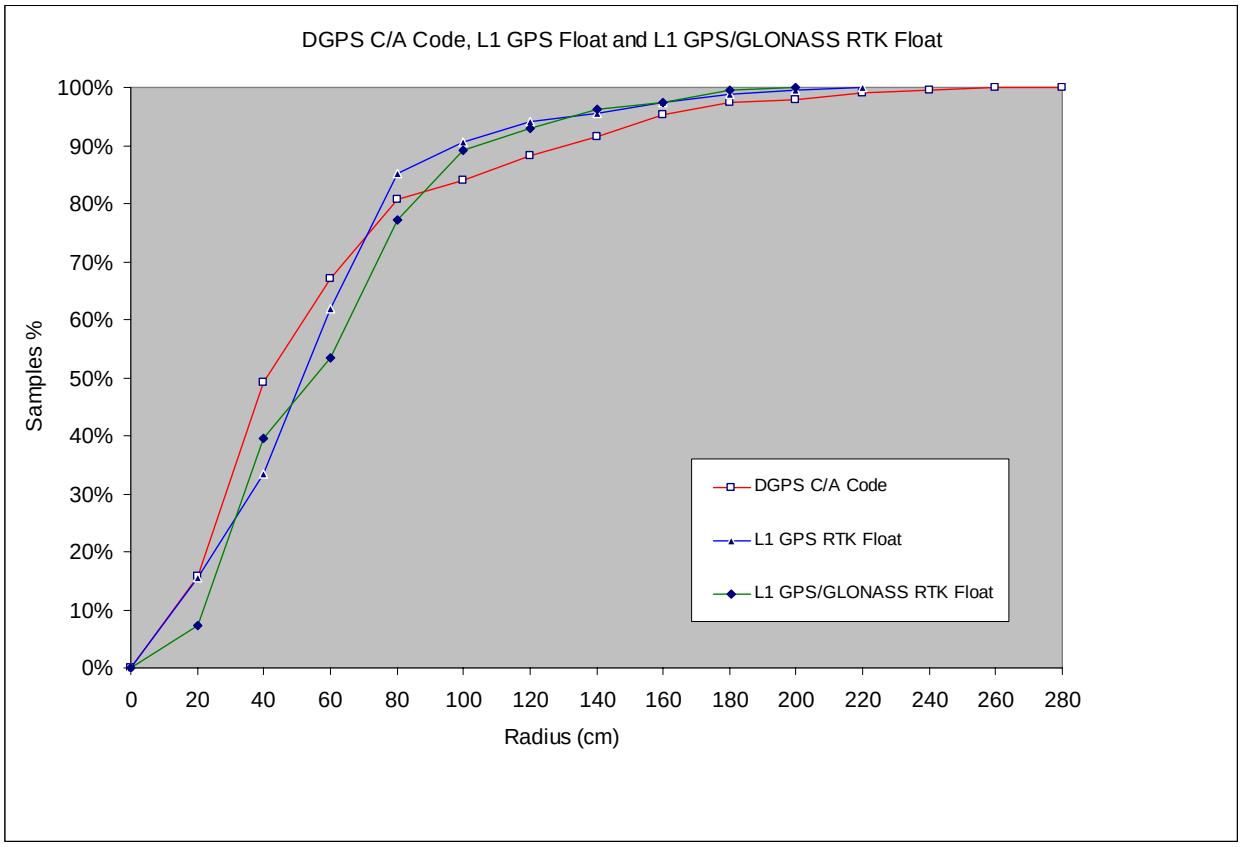

Figure 27 DGPS C/A Code, L1 GPS Float and L1 GPS/GLONASS RTK Float

Figure 28 shows the comparison between the GPS single frequency and the GPS dual frequency. As expected the GPS dual frequencies achieved better accuracy than the single frequency. The advantage of dual frequency is not really that much (only 2.5 cm at 95 % of the samples), but the GPS single frequency couldn't achieve RTK fixed status for long time and was dropping to RTK float. This may be due to the need for more satellites in view or another frequency to fix the RTK solution.

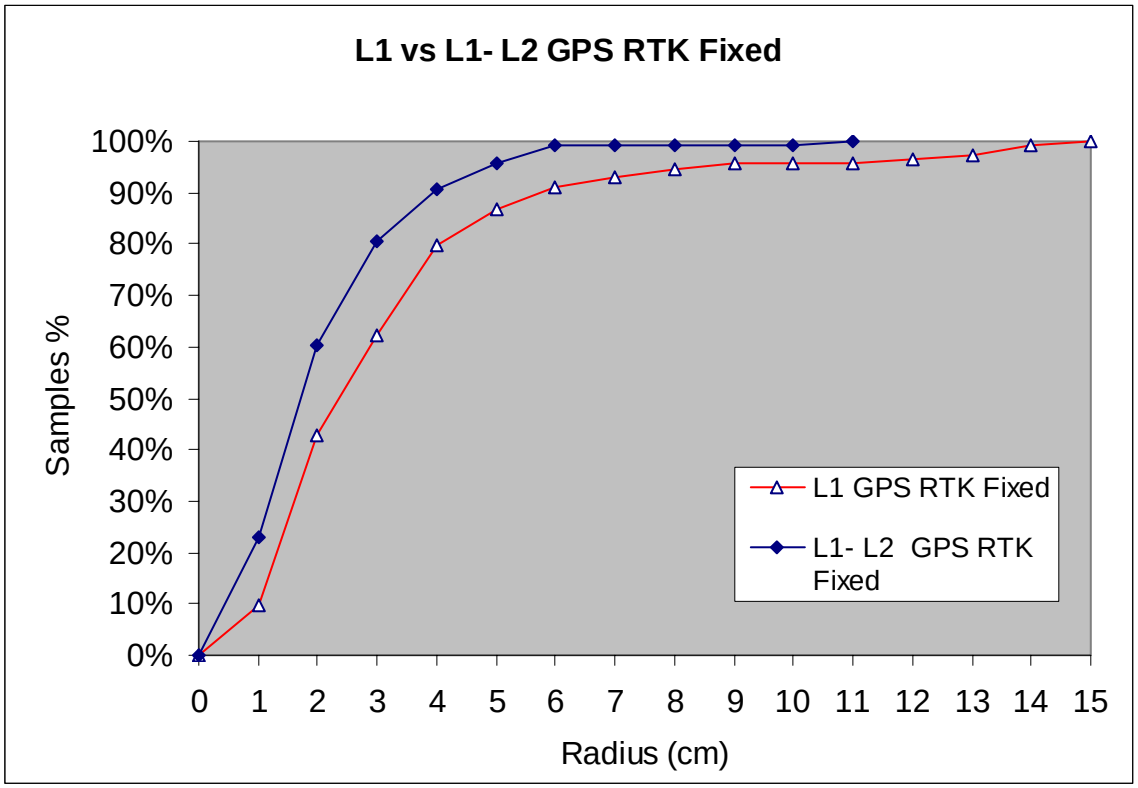

Figure 28 L1 vs. L1-L2 GPS RTK Fixed

Figure 29 demonstrates the comparison between the single system single frequency and the dual system single frequency. The results were exactly as expected; it showed the better accuracy with the use of dual system over the single system.

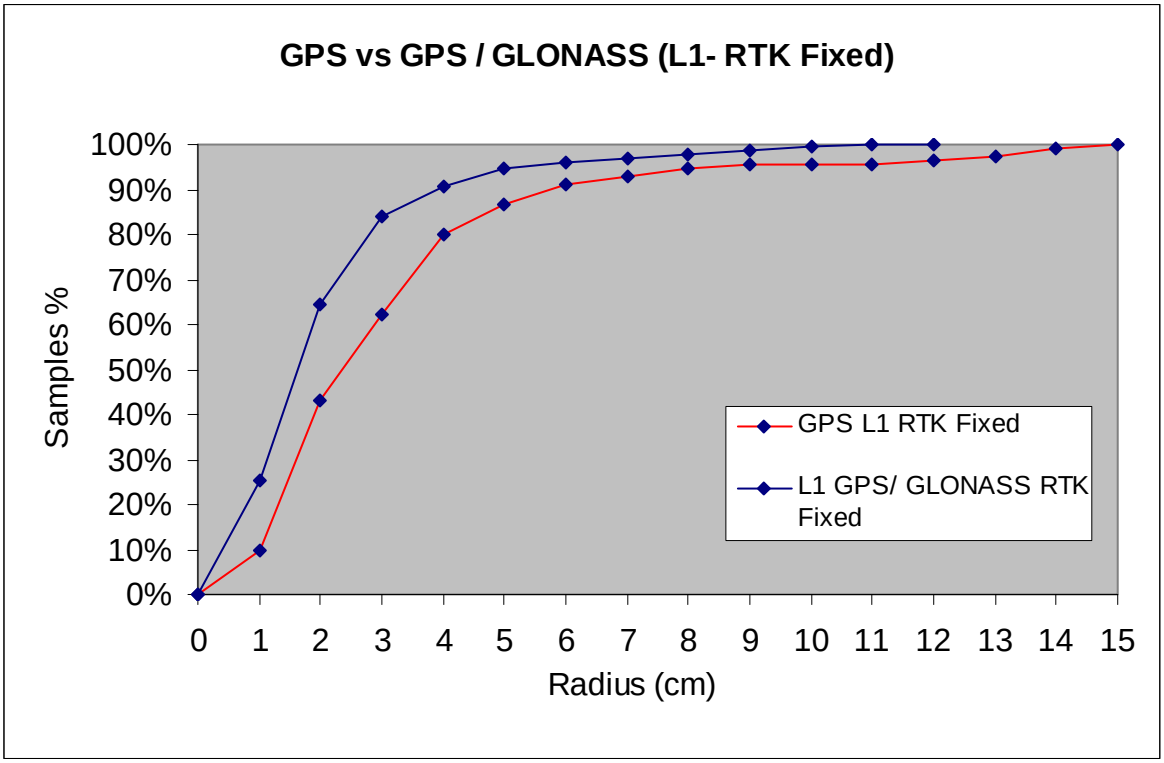

Figure 29 GPS vs. GPS/GLONASS (L1 RTK Fixed)

Figure 30 shows the comparison between GPS dual frequencies against GPS/GLONASS dual frequencies. The two curves almost appear as one. This was not expected because the dual system and dual frequencies should have better accuracy. This may be attributed to the lack of GLONASS satellite in view and the availability of many GPS satellites.

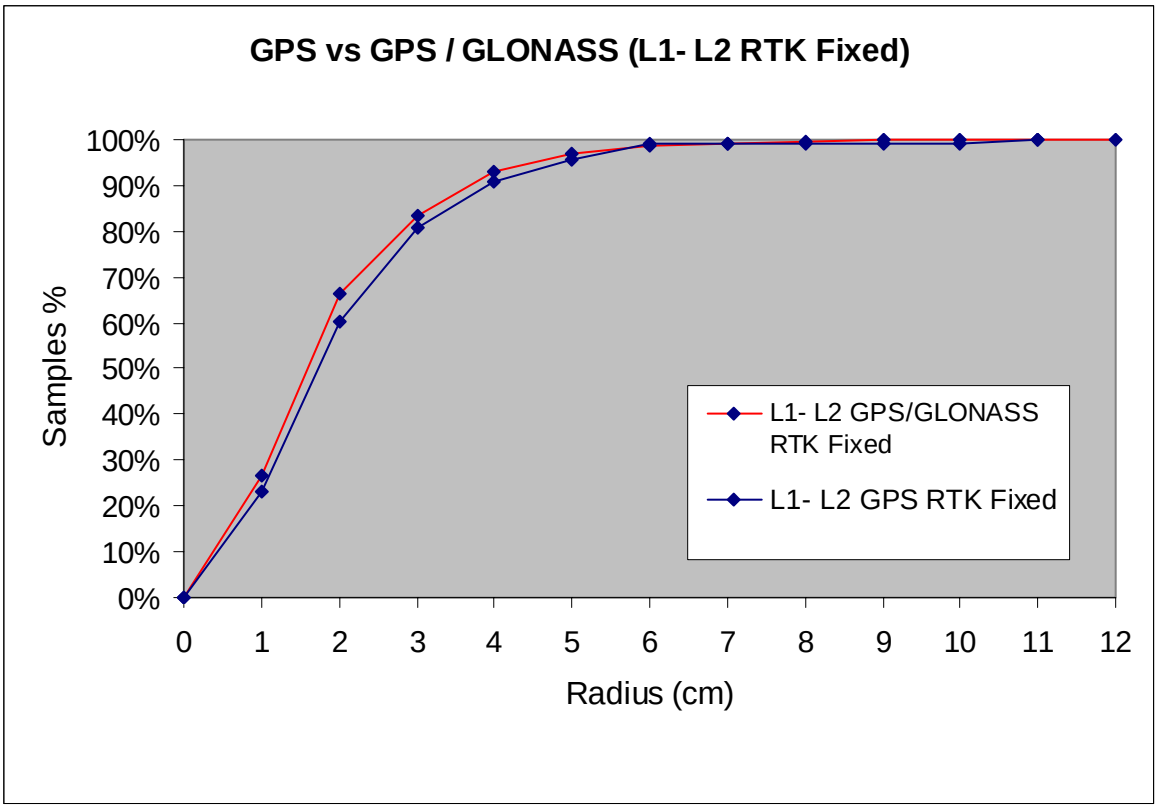

Figure 30 GPS vs. GPS/GLONASS (L1-L2 RTK Fixed)

4.2 Infrared Camera Test Results

Figures 31 to 38 show the infrared cam test results. Each of these figures is the processed output image by crack detection software (WiseCrax®). The detected cracks are marked in red on top of each image. A table that shows the length and width of each crack is attached to the image. Two images have been demonstrated for each moving speed. The considered speeds are 20 mph, 30 mph, 40 mph and 50 mph.

Figure 31- 32 show images taken by the IR camera at speed 20 mph. It is observed that part the crack at the shaded area was detected.

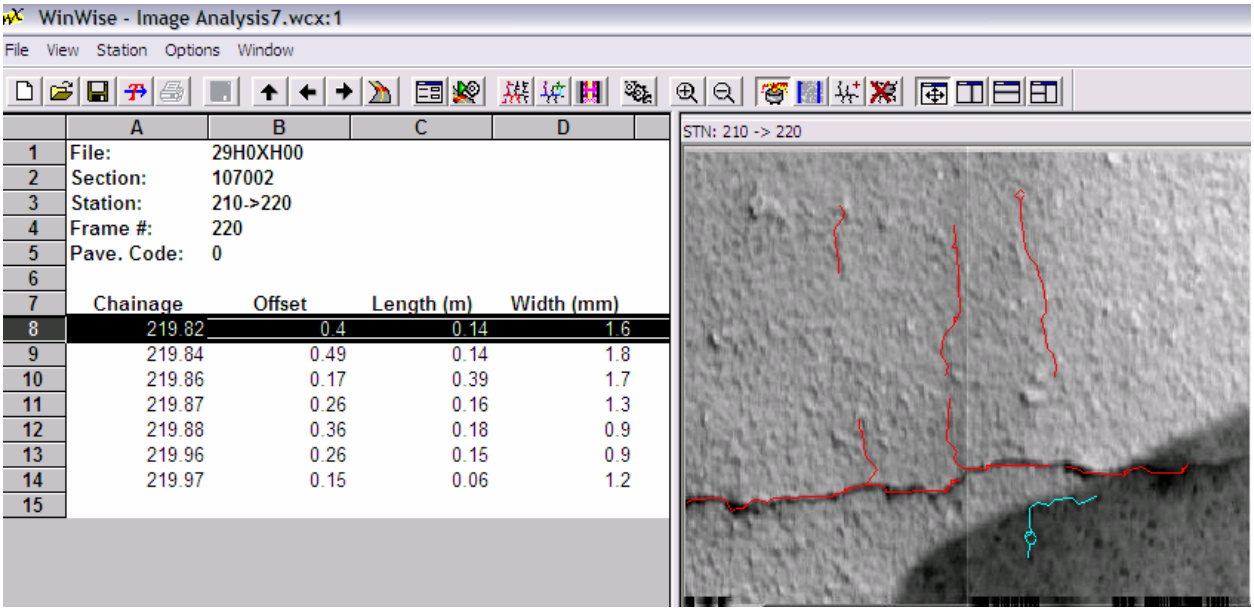

	A	B	C	D
1	File:	29H0XH00		
2	Section:	107002		
3	Station:	210->220		
4	Frame #:	220		
5	Pave. Code:	0		
6				
7	Chainage	Offset	Length (m)	Width (mm)
8	219.82	0.4	0.14	1.6
9	219.84	0.49	0.14	1.8
10	219.86	0.17	0.39	1.7
11	219.87	0.26	0.16	1.3
12	219.88	0.36	0.18	0.9
13	219.96	0.26	0.15	0.9
14	219.97	0.15	0.06	1.2
15				

Figure 31: WiseCrax® Output for Affected Area (image was taken at 20 mph)

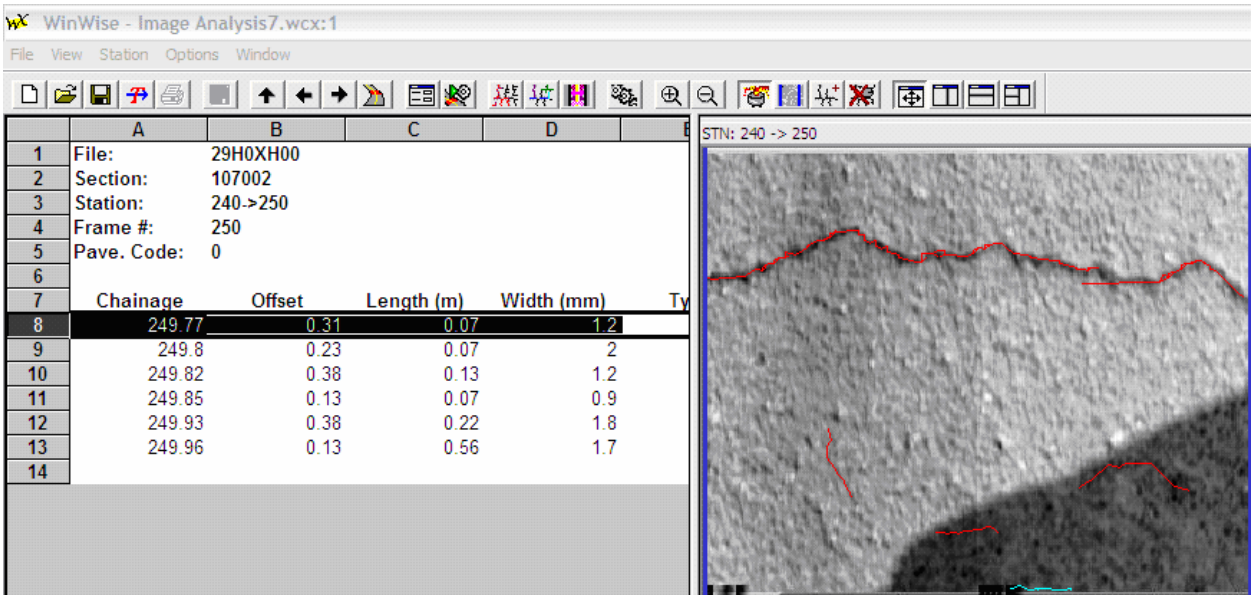

	A	B	C	D
1	File:	29H0XH00		
2	Section:	107002		
3	Station:	240->250		
4	Frame #:	250		
5	Pave. Code:	0		
6				
7	Chainage	Offset	Length (m)	Width (mm)
8	249.77	0.31	0.07	1.2
9	249.8	0.23	0.07	2
10	249.82	0.38	0.13	1.2
11	249.85	0.13	0.07	0.9
12	249.93	0.38	0.22	1.8
13	249.96	0.13	0.56	1.7
14				

Figure 32: WiseCrax® Output for Affected Area (image was taken at 20 mph)

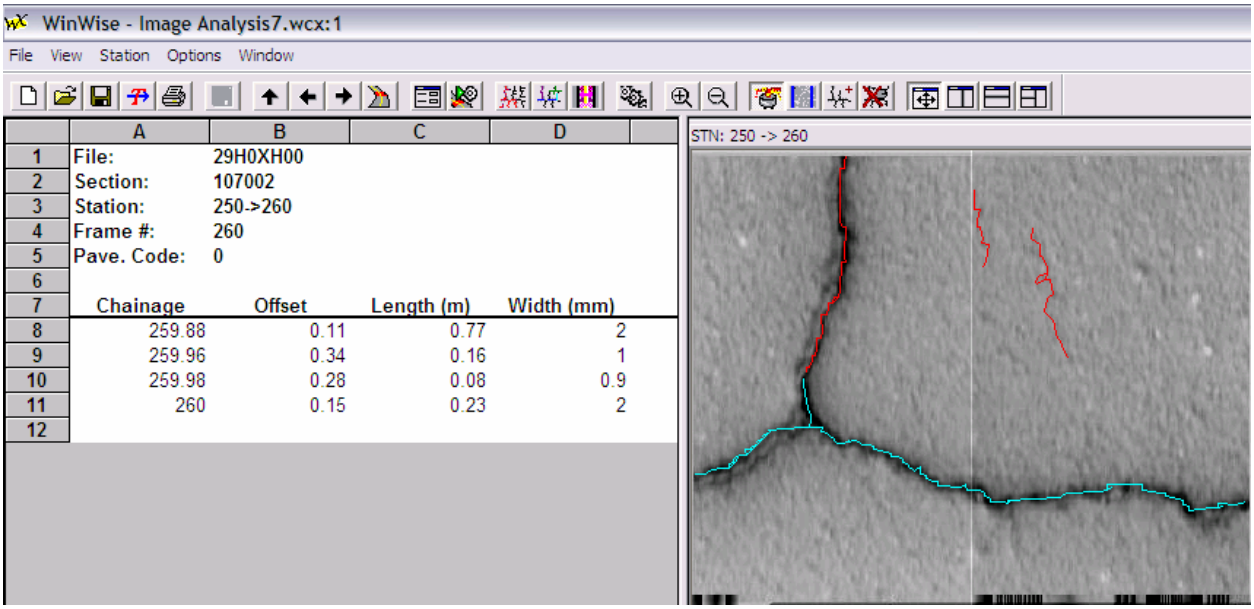

	A	B	C	D
1	File:	29H0XH00		
2	Section:	107002		
3	Station:	250->260		
4	Frame #:	260		
5	Pave. Code:	0		
6				
7	Chainage	Offset	Length (m)	Width (mm)
8	259.88	0.11	0.77	2
9	259.96	0.34	0.16	1
10	259.98	0.28	0.08	0.9
11	260	0.15	0.23	2
12				

Figure 33: WiseCrax® Output for Affected Area (image was taken at 30 mph)

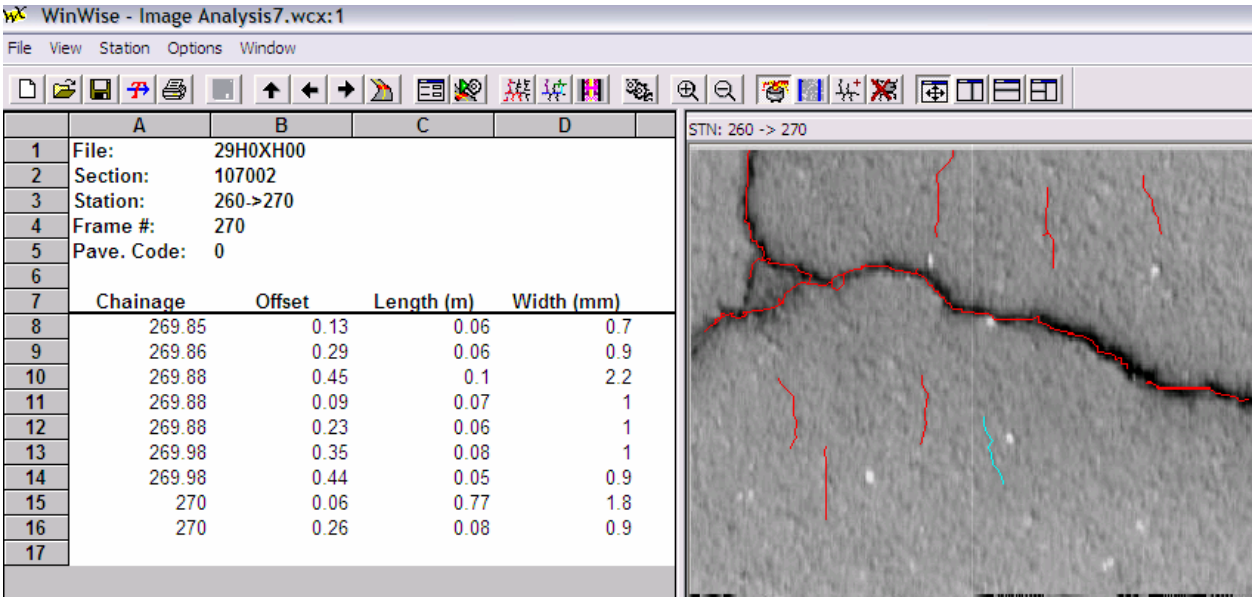

	A	B	C	D
1	File:	29H0XH00		
2	Section:	107002		
3	Station:	260->270		
4	Frame #:	270		
5	Pave. Code:	0		
6				
7	Chainage	Offset	Length (m)	Width (mm)
8	269.85	0.13	0.06	0.7
9	269.86	0.29	0.06	0.9
10	269.88	0.45	0.1	2.2
11	269.88	0.09	0.07	1
12	269.88	0.23	0.06	1
13	269.98	0.35	0.08	1
14	269.98	0.44	0.05	0.9
15	270	0.06	0.77	1.8
16	270	0.26	0.08	0.9
17				

Figure 34: WiseCrax® Output for Affected Area (image was taken at 30 mph)

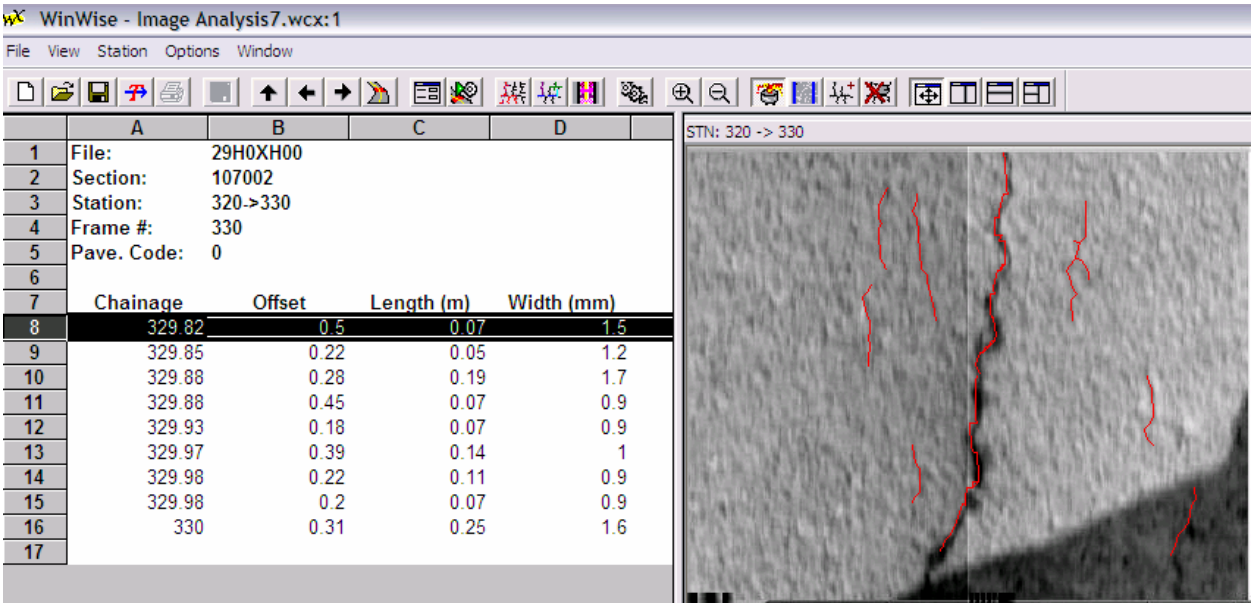

	A	B	C	D
1	File:	29H0XH00		
2	Section:	107002		
3	Station:	320->330		
4	Frame #:	330		
5	Pave. Code:	0		
6				
7	Chainage	Offset	Length (m)	Width (mm)
8	329.82	0.5	0.07	1.5
9	329.85	0.22	0.05	1.2
10	329.88	0.28	0.19	1.7
11	329.88	0.45	0.07	0.9
12	329.93	0.18	0.07	0.9
13	329.97	0.39	0.14	1
14	329.98	0.22	0.11	0.9
15	329.98	0.2	0.07	0.9
16	330	0.31	0.25	1.6
17				

Figure 35: WiseCrax® Output for Affected Area (image was taken at 40 mph)

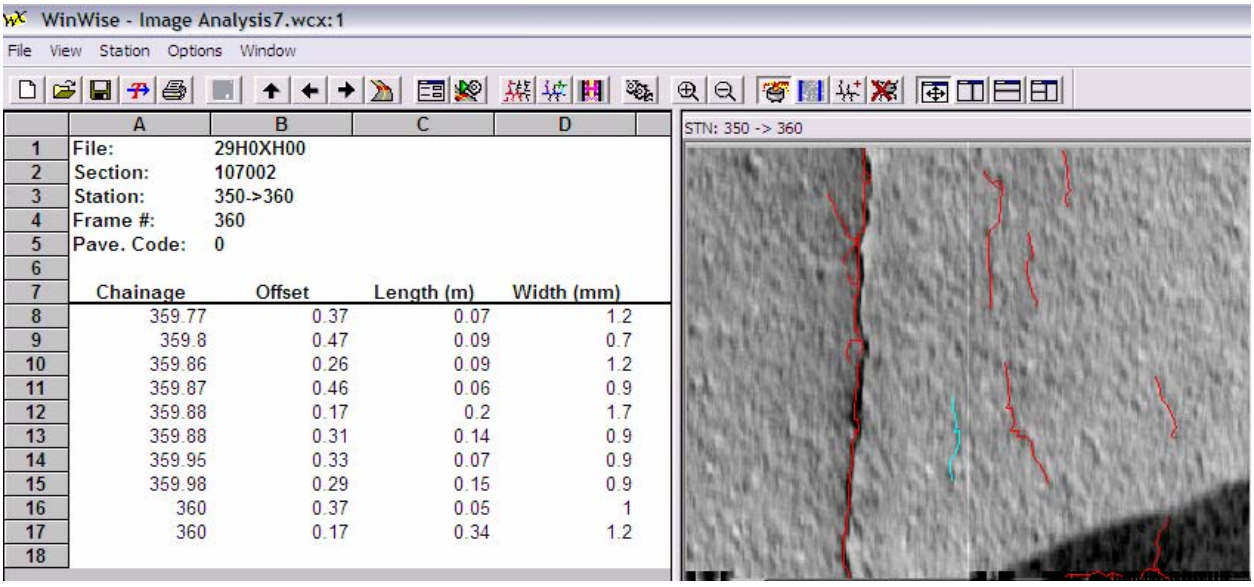

	A	B	C	D
1	File:	29H0XH00		
2	Section:	107002		
3	Station:	350->360		
4	Frame #:	360		
5	Pave. Code:	0		
6				
7	Chainage	Offset	Length (m)	Width (mm)
8	359.77	0.37	0.07	1.2
9	359.8	0.47	0.09	0.7
10	359.86	0.26	0.09	1.2
11	359.87	0.46	0.06	0.9
12	359.88	0.17	0.2	1.7
13	359.88	0.31	0.14	0.9
14	359.95	0.33	0.07	0.9
15	359.98	0.29	0.15	0.9
16	360	0.37	0.05	1
17	360	0.17	0.34	1.2
18				

Figure 36: WiseCrax® Output for Affected Area (image was taken at 40 mph)

Figure 37- 38 show images taken by the IR camera at speed 50 mph. It was noticed that not all the cracks have been detected but the majority was identified. This indicates the clarity of the images decrease with the increase of vehicle speed.

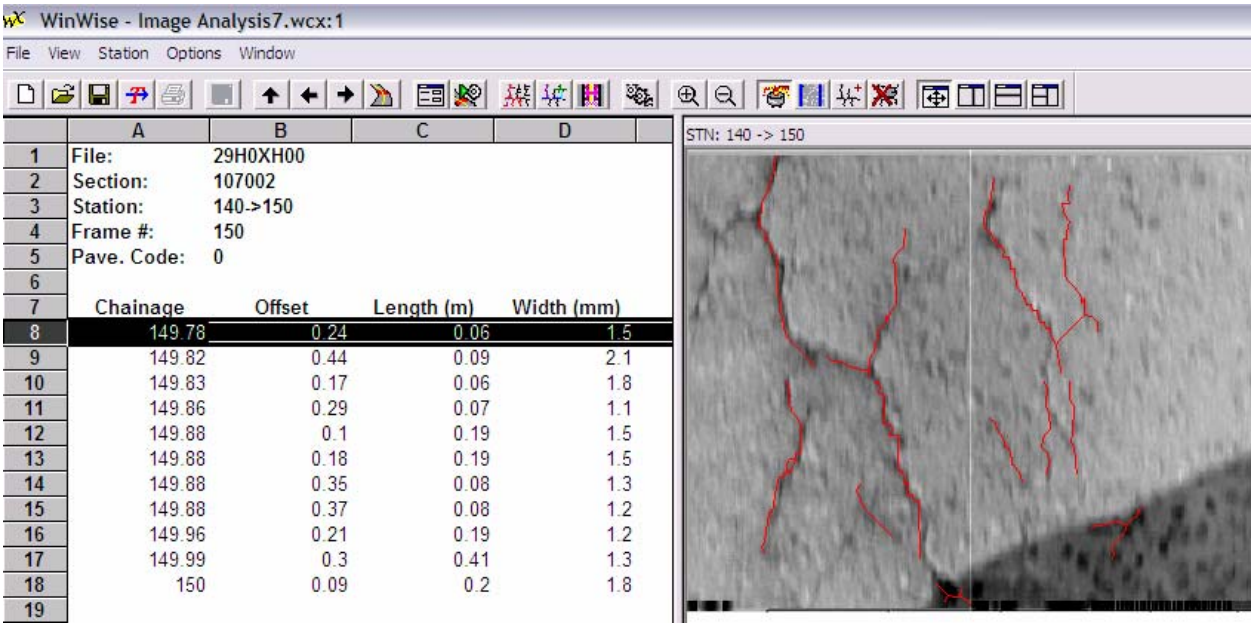

	A	B	C	D
1	File:	29H0XH00		
2	Section:	107002		
3	Station:	140->150		
4	Frame #:	150		
5	Pave. Code:	0		
6				
7	Chainage	Offset	Length (m)	Width (mm)
8	149.78	0.24	0.06	1.5
9	149.82	0.44	0.09	2.1
10	149.83	0.17	0.06	1.8
11	149.86	0.29	0.07	1.1
12	149.88	0.1	0.19	1.5
13	149.88	0.18	0.19	1.5
14	149.88	0.35	0.08	1.3
15	149.88	0.37	0.08	1.2
16	149.96	0.21	0.19	1.2
17	149.99	0.3	0.41	1.3
18	150	0.09	0.2	1.8
19				

Figure 37: WiseCrax® Output for Affected Area (image was taken at 50 mph)

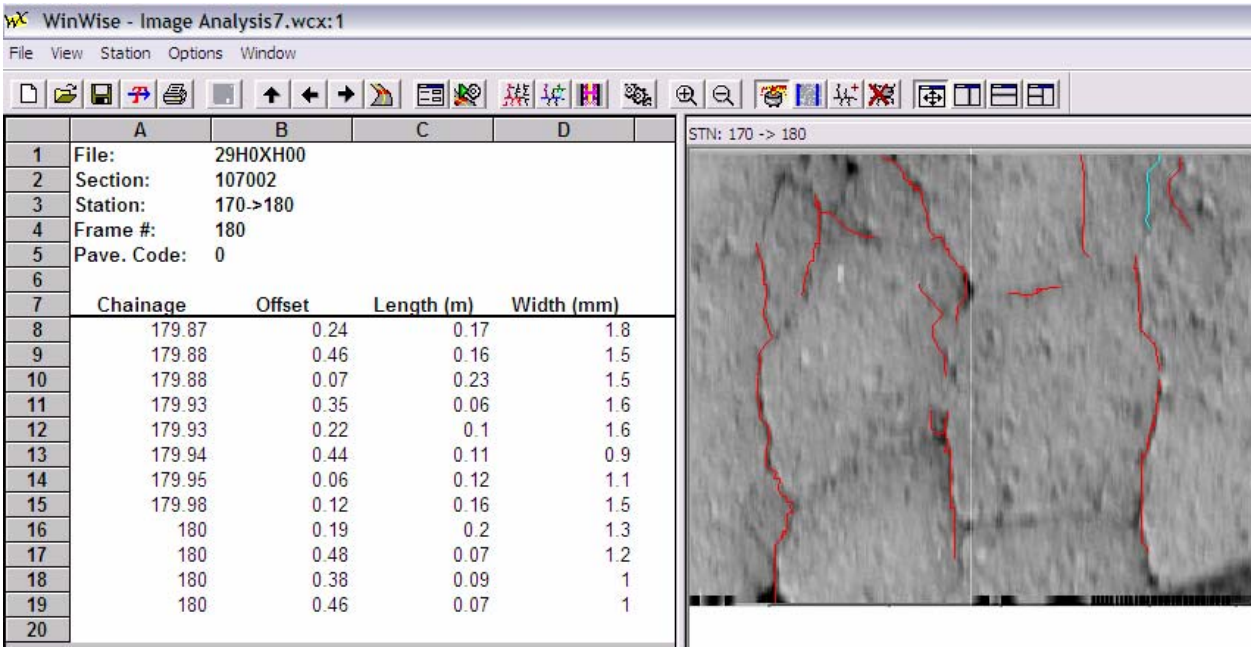

	A	B	C	D
1	File:	29H0XH00		
2	Section:	107002		
3	Station:	170->180		
4	Frame #:	180		
5	Pave. Code:	0		
6				
7	Chainage	Offset	Length (m)	Width (mm)
8	179.87	0.24	0.17	1.8
9	179.88	0.46	0.16	1.5
10	179.88	0.07	0.23	1.5
11	179.93	0.35	0.06	1.6
12	179.93	0.22	0.1	1.6
13	179.94	0.44	0.11	0.9
14	179.95	0.06	0.12	1.1
15	179.98	0.12	0.16	1.5
16	180	0.19	0.2	1.3
17	180	0.48	0.07	1.2
18	180	0.38	0.09	1
19	180	0.46	0.07	1
20				

Figure 38: WiseCrax® Output for Affected Area (image was taken at 50 mph)

5. SUMMARY AND CONCLUSION

Asphalt crack detection is a fundamental issue for road management and maintenance. Over the past two decades there have been many trials to develop accurate and reliable automated crack detection systems. Nowadays, there are many automated systems; however, these systems generally have some deficiencies:

1. The image acquisition in these systems is done by utilizing digital or analogue cameras. These cameras fail to detect some types of cracks (white cracks and perpendicular cracks to the roadway). In addition, they require explicit amount of light to function properly and work only under certain weather condition.
2. The exact location of the cracks is not recorded in a way that makes it easy to locate.

The recent developed technologies such as GPS and infrared cameras can help in this area. The GPS technology can help in the area of precise location. It can give accuracy up to sub-centimeter level. The infrared technology depends on the heat emitted from an object with the consideration that cracks and healthy asphalt have different emissivity. It also doesn't need visible light, and it is able to operate under most weather conditions.

This research has proven that infrared camera can capture images up to 50 mph that can be analyzed by crack detection software. Cracks up to 1 mm width are detected regardless to the crack color or contrast. The IR camera also didn't require any additional light to operate. The research also suggested an integrated system that can include the images of cracks and its position using the GPS system.

The following conclusions can be reached from the GPS/ GLONASS test and infrared camera test:

1- The GPS system is well developed. The number of satellites that were in view during the test ranged between 6-11 satellites; which assist in more reliable and accurate location calculation.
2- The GLONASS system is declining. The number of satellites that were in view during the test ranged between 0 and 3 satellites.
3- The GPS and GLONASS receivers gave almost the same accuracy as the GPS only receivers. This is because the GLONASS satellites were not always in view.
4- The GPS/GLONASS receivers may achieve better accuracy level in open areas where no obstacles around (freeways) but inside the city, the GLONASS satellites have almost no effect on the receiver readings (Trimble planning showed GLONASS satellites that couldn't be detected by receiver due to the surrounding buildings).
5- The GPS single frequency in RTK fixed mode achieved almost the same accuracy as the GPS dual frequency receivers in RTK mode, however, it takes longer time to achieve the RTK fixed mode and it drops frequently to RTK float (Javad model) which is less accurate than the RTK fixed mode.
6- The integration time in infrared cameras plays an important role in the clarity of the images taken in real time. The integration time should be adjusted according to the pavement temperature (by several trails and errors) to have clear images.
7- The infrared camera gave high quality real time images at speeds ranging from 20 up to 50 mph. However, at 50 mph it gave slightly less lucid images than at 20-40 mph. At 60 mph the images were blurry and almost impossible to detect by crack detection software.

The following recommendations should be considered in any further investigation for the use of infrared camera for asphalt crack detection:

1- The effects of using wide-angle lens and raising the distance between the asphalt surface and the camera (so that the taken images would cover the whole lane width) on the clarity of the image.

2- Investigating if the changes of the integration time in IR camera have any affect one the traveling speed and also studying the suitable integration time for the various temperatures thought the different parts of the day.

LIST OF REFERENCES

1. AASHTO, 2001. "Quantifying Cracks in Asphalt Pavement Surface." Designation PP44- 01, American Association of State Highway Officials, Washington D.C., 2000.

2. Abousalem, M.A. "Development and Analysis of Wide Area Differential GPS Algorithms" UCGE Reports Number 20083, Department of Geomantic Engineering, The University of Calgary, AB, Canada 1996.

3. Alt, David G. and David A. Meggers. "Determination of Bridge Deck Subsurface Anomalies by Infrared Thermography and Ground Penetrating Radar." Polk Viaduct I-70, Topeka, Kansas. Report for Kansas Department of Transportation. September 1996.

4. Balaras, C.A. and Argiriou, A.A. "Infrared Thermography for Building Diagnostics." Energy and Buildings, Vol. 34 No.2 (2002).

5. Dana, P. H. "Global Positioning System Overview." TX, 1998. http://www.ncgia.ucsb.edu/education/curricula/giscc/units/u017/u017.html.

6. El-Rabbany, Ahmed." Introduction to GPS." Boston, MA: Artech House, Inc., 2002.

7. Gary Shubinsky. "Visual & Infrared Imaging for Bridge Inspection." Northwestern University BIRL Basic Industrial Research Laboratory. Report, June 1994.

8. GIS Development Pvt. Ltd. "http://www.gisdevelopment.net/tutorials/tuman004pf.htm". Accessed on April 2005.

9. "GPS Fundamentals & Applications" Arlington: VA, Navtech Seminars, Inc., 1996.

10. Gunaratne, M., I. Sokolic, A. Mraz, A. Nazef. "Evaluation of Pavement Distress Imaging Systems." Transportation Research Board, TRB, 2004.

11. Hunag, Yang H. "Pavement Analysis and Design." Upper Saddle River, NJ: Prentice Hall. 1993.

12. Hurn, J. "Differential GPS Explained." Sunnyvale: CA, Trimble Navigation, Ltd., 1993.

13. Javad Navigation Systems, "http://www.javad.com." Accessed on April 2005.

14. NASA's Infrared Processing and Analysis Center (IPAC). California Institute of Technology. Pasadena, CA. http://www.ipac.caltech.edu/Outreach/Edu/infrared.html

15. Oloufa, AA; Mahgoub, HS; Ali, H. "*Infrared* Thermography for Asphalt Crack Imaging and Automated Detection." Transportation Research Board, TRB, 2004.

16. Oloufa, A., W. Do and R. Thomas. "Automated Monitoring Compaction Using GPS." Proceedings of the ASCE Annual Convention and Construction Congress. Oct. 1997.

17. Roberts, G.W., Meng X., and A. H. Dodson. "Integrating a Global Positioning System and Accelerometers to Monitor the Deflection of Bridges." Journal of Surveying Engineering 130.2 ,2004.

18. Shanks, Brian (POC), "Infrared Thermography for Roof Leaks." Department of Energy, Oak Ridge Operations - Oak Ridge, TN, December 1999.

19. Shin, Heejeong, FNU Brawijaya and Kimberly Belli. "Sensor Fusion for Bridge Deck and Pavement Evaluation" CenSSIS Research and Industrial Collaboration Conference. Northeastern University, Boston, Massachusetts. January 29-30, 2002.

20. Wang K. C. P, R. P. Elliott "Investigation of Image Archiving for Pavement Surface Distress Survey." July 26, 1999.

21. Wang, K.C.P. "Designs and Implementations of Automated Systems for Pavement Surface Distress Survey." Journal of Infrastructure Systems, ASCE, Vol. 6, No. 1, March, 2000.

22. Washer, Glenn A. "Developing NDE Technologies for Infrastructure Assessment." Public Roads Journal, No. 4, Jan. 2000.

23. WiseCrax® Asphalt Crack Detection Software Version 3.04, Roadware Inc., Ontario, Canada. February 2003.